

國立臺灣大學電機資訊學院電子工程學研究所



碩士論文

Graduate Institute of Electronics Engineering
College of Electrical Engineering & Computer Science
National Taiwan University
Master Thesis

以光體積描述訊號偵測心房顫動之
快速篩檢與長期監測應用

Robust PPG-based Atrial Fibrillation Detection with
Applications to Fast Screening and Long-term Monitoring

山仕明

Shih-Ming Shan

指導教授：吳安宇博士

Advisor: An-Yeu Wu, Ph.D.

中華民國 106 年 4 月

April, 2017





國立臺灣大學碩士學位論文
口試委員會審定書

以光體積描述訊號偵測心房顫動之

快速篩檢與長期監測應用

Robust PPG-based Atrial Fibrillation Detection with
Applications to Fast Screening and Long-term Monitoring

本論文係山仕明君 (R03943004) 在國立臺灣大學電子工程學研究所完成之碩士學位論文，於民國 106 年 4 月 14 日承下列考試委員審查通過及口試及格，特此證明

口試委員：

吳安宇

(指導教授)

楊家張

賴達明

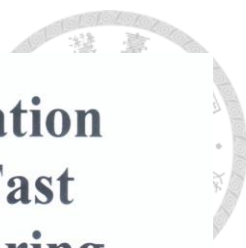
湯頌忠

古博文

系主任、所長

吳安宇





Robust PPG-based Atrial Fibrillation Detection with Applications to Fast Screening and Long-term Monitoring

By
Shih-Ming Shan

THESIS

Submitted in partial fulfillment of the requirement
for the degree of Master of Science in Electronics Engineering
at National Taiwan University
Taipei, Taiwan, R.O.C.

April 2017

Approved by:

Chia-Hsiang Yang Chia-Hsiang Yang Angchen Ly
Dainy Lai Ku, Po Wen

Advised by:

Chia-Hsiang Yang

Approved by Director:

Chia-Hsiang Yang



致謝



兩年來的碩士生活即將畫上句點，能夠順利畢業，心中充滿感激。首先要謝謝我的指導教授吳安宇博士，老師豐富的學識及嚴謹的態度，讓我不論是在研究上或生活處事上都獲益良多。感謝計畫主持人湯頌君醫師、賴達明醫師細心指導跨領域的相關知識，並不厭其煩的解答我的疑惑。很榮幸請到湯頌君醫師、賴達明醫師、楊家驥教授和古博文經理來擔任我的口試委員，感謝各位委員在口試時給予的指導與改正，讓本論文更完整。

感謝實驗室的夥伴們，因為有你們帶來融洽歡樂的氣氛，辛苦的研究生活也變得豐富有趣：感謝李宗翰、林祐民、黃珮雯、黃韋翰、陳柏宏、鄭宏毅、蔡承融、李懷霆、李鼎元、吳秉宸、魏旻良、曾煥富、劉祐成、陳奕、陳毓茵、洪偉倫、朱瑋晴和劉佳琛等實驗室學長姊的照顧以及研究上的指引；謝謝陳敬恆、廖經群、陳庭笙、周敬堯、高聖鈞、吳佳衡、郭泓圻、劉佑新和蔡孟亞等同學的扶持與砥礪，一同修課、熬夜寫作業、做研究，很開心能和你們一同努力度過這兩年時光；謝謝王聖輝、陳政文、侯凱倪、汪敬哲等學弟妹的幫忙與協助。也感謝實驗室助理邱玉霜幫我們處理實驗室事務。

感謝我的父母、家人、女友及朋友對我的照顧、關心以及包容，使我能專心於學術研究，樂觀的面對每次生活或是研究上的挫折與不順利。最後，謹以此論文獻給所有關心我的師長、家人和朋友，以及一路上每位幫助過我的人。

山仕明 謹誌

於台大電子所 Access IC 實驗室

中華民國 106 年 4 月 17 日



摘要



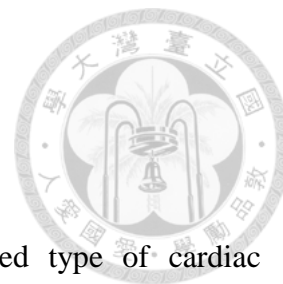
心房顫動是一種因為心臟內產生節律訊號的功能異常，是最常見的心臟節律異常疾病，由於心房顫動亦是提高中風風險約五倍的危險因素，所以自動偵測心房顫動是一個重要的醫學議題，對於包含一般民眾的篩檢，以及疑似心房顫動的病患之長期監測而言。目前最有效的診斷為心電圖，然而，各種心電圖儀器都有一些缺點，例如，需要一邊肢體至少一個電極、或費用較高。另一方面，使用光體積描述訊號的偵測方式值得深入探討，光體積描述訊號是一種由血氧機可取得，可反應心律之信號。相較於心電圖較為簡便，因此，更適合長期監測病人生理訊號，並偵測像心房顫動等具有陣發性之心臟節律異常疾病。

然而，本論文中提到的以光體積描述訊號偵測心房顫動之現有相關著作，除了資料測量環境較標準化外，缺點多為較少考慮基線飄移，只考量單一的訊號參數序列等前處理問題，與較無探討特徵抽取的多寡與選取以及學習等後處理問題。因此，本論文提出一個以光體積描述訊號偵測心房顫動的架構，並且探討實際臨床應用上快速篩檢與長期監測的不同需求。在臺大醫院提供的實際臨床生理訊號資料中，本論文提出之架構之接收者操作特徵曲線的曲線下面積，靈敏度，特異度與準確度分別達到 98.0%，95.4%，97.9%與 97.3%，該數據較現有的光體積描述訊號偵測心房顫動之相關著作良好，且跟心電圖的心房顫動偵測架構準確度接近，並且在快速篩檢的應用上，可以將量測時間縮短至 30 秒並只增加少量的誤差，這說明本論文提出之光體積描述訊號架構有潛力被使用在快速篩檢與長期監測心房顫動。

關鍵字：心房顫動、光體積描述訊號、特徵抽取、基因演算法、快速篩檢



Abstract



Atrial Fibrillation (AF) is the most common and sustained type of cardiac arrhythmia. Since AF is a risk factor for stroke, automatic detection of AF is an important public health issue. Currently, the most useful and accurate tool for diagnosing AF is electrocardiography (EKG). However, EKG monitoring devices have their limitations or drawbacks. On the other hand, photoplethysmogram (PPG) is an alternative technique to obtain the heart rate information by pulse oximetry. Compared with EKG monitors, PPG devices are more convenient, making PPG promising in identifying paroxysmal AF.

The aim of this thesis is to investigate the potential of analyzing PPG waveforms to identify patients with AF. The state-of-the-art PPG-based AF detection researches in this thesis have some limitations. In addition, there is still performance gap between related works and EKG-based algorithm. Therefore, we propose a PPG-based AF detection framework, including pre-processing, feature extraction, and SVM classification with GA-based optimization. The receiver operating characteristic curve (ROC) and statistical measures were applied to evaluate model performances. Furthermore, two clinical scenarios, long-term monitoring and fast screening were considered in the experiments. Among 673 patients' signals recorded in clinic

environments, we achieve ROC area under curve, sensitivity, specificity and accuracy of 0.980, 0.954, 0.979 and 0.973, respectively. And the record time can be shorten to 30 seconds with little performance degradation in fast screening scenario. The result suggests that the PPG-based AF detection algorithm is a promising pre-screening tool for AF and helps doctors monitoring patient with arrhythmia.

Keywords: Atrial Fibrillation, Photoplethysmogram, Feature extraction, Genetic algorithm, Screening

Contents

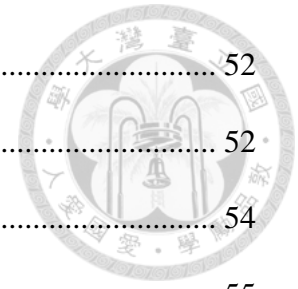


致謝	v
摘要	vii
Abstract.....	ix
Contents.....	xi
List of Figures.....	xiv
List of Tables	xviii
Chapter 1 Introduction and Motivation.....	1
1.1 Overview of Atrial Fibrillation (AF).....	1
1.1.1 Symptoms and Effects of AF.....	1
1.1.2 Current diagnosis of AF.....	3
1.2 Motivation and Contribution of PPG-based AF Detection.....	6
1.2.1 Introduction of PPG signal	7
1.2.2 Motivation and Contribution	7
1.3 Thesis Organization	10
Chapter 2 Related Works of AF Detection.....	12
2.1 AF Detection algorithms	12
2.1.1 EKG-based AF detection.....	12
2.1.2 PPG-based AF detection.....	14
2.2 AF Detection Application: Fast-screening and Long-term Monitoring .	18



2.2.1	Long-term monitoring AF detection.....	18
2.2.2	Fast screening AF detection.....	19
2.3	Summary.....	21
Chapter 3	Pre-processing and Feature Extraction of PPG-based AF Detection	23
3.1	PPG-based AF Detection Framework	23
3.2	Data Collection.....	25
3.3	Pre-processing with Baseline Removal	27
3.3.1	Baseline wandering in PPG signals and its effects on AF detection 27	
3.3.2	State-of-the-art baseline removal algorithms	28
3.3.3	Proposed MMF-based Pre-processing.....	32
3.4	Feature Extraction.....	35
3.4.1	Time domain and frequency domain features	35
3.4.2	Entropy domain features.....	37
3.5	Statistical Analysis.....	42
3.6	Summary.....	44
Chapter 4	Classification and Optimization of PPG-based AF Detection.....	45
4.1	Feature Selection	45
4.2	Classification	47
4.2.1	Classification and parameter tuning	47
4.2.2	Performance and summary of traditional solution	50
4.2.3	Limitations in traditional solution	51
4.3	Features and Classifier Parameters Optimization with GA-based	

Algorithms.....	52
4.3.1 Introduction to GA Algorithms.....	52
4.3.2 Optimization with GA Algorithms	54
4.4 Results of the PPG-based AF Detection Framework.....	55
4.4.1 Performance comparisons.....	55
4.4.2 Features selected in the proposed framework.....	57
4.4.3 Validation within ICU data	57
4.5 Summary.....	59
Chapter 5 Application of PPG-based AF Detection.....	60
5.1 Results of Application: Fast Screening and Long-term Monitoring	60
5.1.1 Fast screening	60
5.1.2 Long-term monitoring	62
5.2 Validation on MTK Device	66
5.3 Implementation of Graphic User Interface.....	67
5.4 Summary.....	70
Chapter 6 Conclusion and Future Works	71
6.1 Main Contribution	71
6.2 Future Works	72
Reference	74



List of Figures



Fig. 1.1 Heart activity of (a) Normal sinus rhythm (NSR), and (b) Atrial fibrillation (AF) [2]..... 2

Fig. 1.2 (a) Holter monitoring. (b) Patient-triggered event monitor (c) Patient monitor (d) Implantable loop recorder (e) Mobile cardiovascular telemetry [1] [2] [8] [13] 5

Fig. 1.3 Example of a photoplethysmographic waveform [12]..... 7

Fig. 1.4 PPG devices of (a) Pulse oximetry, and (b) Wrist-type PPG sensor watch [13] 8

Fig. 1.5 PPG and EKG signals with (a) normal sinus rhythm (NSR), and (b) AF 9

Fig. 1.6 (a) The concept of fast screening AF detection, and (b) Confusion matrix 10

Fig. 1.7 (a) The concept of long-term monitoring AF detection, and (b) An example of long-term monitoring..... 10

Fig. 2.1 iPhone 4S prototype for AF detection [18] 15

Fig. 2.2 The flow chart of testing [19]..... 16

Fig. 2.3 The percentage of detected AF when the duration of EKG monitoring is



prolonged [7] 19

Fig. 2.4 Smartphone camera-based PPG measurements (A) The Cardio Rhythm standalone smartphone application. (B) Example of measurement. (C) Examples of PPG recordings from normal sinus rhythm. (D) Examples of PPG recordings from an AF patient [14] 21

Fig. 3.1 The flowchart of related work [20] 24

Fig. 3.2 The flowchart of the proposed framework 25

Fig. 3.3 Extracted parameters of (a) PPG, and (b) EKG 27

Fig. 3.4 PPG waveforms and the effect of baseline 28

Fig. 3.5 The waveform processed by the FIR filter 29

Fig. 3.6 PPG de-trend using empirical mode decomposition 30

Fig. 3.7 The waveform processed by the EEMD 31

Fig. 3.8 The basic operators of MMF [32] 31

Fig. 3.9 Applying MMF to PPG signals 32

Fig. 3.10 The flowchart of the proposed pre-processing 33

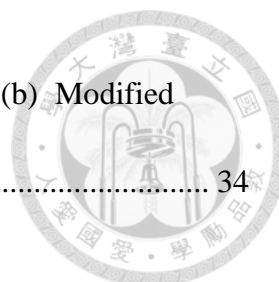


Fig. 3.11 (a) The amplitude of baseline wandering signal, and (b) Modified definition of AMP..... 34

Fig. 3.12 HRV power spectrum over 24 hours [33] 37

Fig. 3.13 The boxplot of (a) Shannon entropy calculated by fixed threshold, and (b) Modified Shannon entropy calculated by fixed group number 39

Fig. 3.14 The boxplot of (a) TPR1, and (b) TPR2..... 40

Fig. 3.15 The p-values of features extracted from PPG (a) PPI - Time domain features, (b) AMP - Time domain features, (c) PPI - Frequency domain features, (d) AMP - Frequency domain features, (e) PPI - Entropy domain features, and (f) AMP - Entropy domain features 43

Fig. 4.1 Flow chart of classification part 45

Fig. 4.2 (a) Concept of feature selection, and (b) Concept of wrapper type feature selection [39] 47

Fig. 4.3 The flow of classification with 5-fold cross-validation 48

Fig. 4.4 Confusion matrix..... 50

Fig. 4.5 The result of grid search..... 51



Fig. 4.6 The simple flow chart of GA algorithms.....	53
Fig. 4.7 The mutation methods.....	53
Fig. 4.8 The chromosomes, solution structure.....	55
Fig. 4.9 The proposed GA-based optimization with cost-sensitive SVM.....	55
Fig. 4.10 ROC curve comparisons	56
Fig. 4.11 The concept of over-fitting test	58
Fig. 5.1 Long-term monitoring result of patient (a) ID=2956355 PPG, (b) ID=2956355 EKG, (c) ID=3234202 PPG, (d) ID=3234202 EKG, (e) ID=5302261 PPG, (f) ID=5302261 EKG, (g) ID=5650186 PPG, and (h) ID=5650186 EKG	65
Fig. 5.2 Adopted from MediaTek. The flow chart of applied MT2511 in validation.....	67
Fig. 5.3 The interface of GUI	68
Fig. 5.4 Report of long-term monitoring	69
Fig. 5.5 Report of fast-screening	69

List of Tables



Table 1-1 The pros and cons of cardiac monitoring devices [8] [10] [11].....	6
Table 2-1 The comparisons of performances in related works [17] [18] [19] [20]	16
Table 2-2 Summary of performance comparisons [14]	20
Table 3-1 Comparisons of related work and proposed frameworks	25
Table 3-2 Performance comparisons of pre-processing.....	34
Table 3-3 All candidate features	41
Table 4-1 Steps of sequential forward selection (SFS) and sequential backward selection (SBS).....	47
Table 4-2 Performance comparisons in traditional solution and related work	51
Table 4-3 The performance comparisons.....	56
Table 4-4 The feature selected in the proposed framework.....	57
Table 4-5 Test set accuracy compared to the optimized accuracy	58
Table 5-1 Performances on different data length.....	61
Table 5-2 The trial validation on MTK devices, MT2511	67



Chapter 1

Introduction and Motivation



1.1 Overview of Atrial Fibrillation (AF)

Atrial Fibrillation (AF) is the most common type of arrhythmia, which is an abnormal heart rhythm characterized by rapid and irregular heart beating [1]. The symptoms and current diagnosis of AF will be introduced in this session.

1.1.1 Symptoms and Effects of AF

Atrial Fibrillation (AF) occurs if rapid, disorganized electrical signals cause the atria to contract irregularly. Normally, with each heartbeat, an electrical signal begins in sinoatrial (SA) node, travels through the right and left atria, making the atria to contract and pump blood into the ventricles. The electrical signal then moves down to atrioventricular (AV) node and allows the ventricles to finish filling with blood [2]. The normal electrical pathways and electrocardiogram (EKG) is shown in Fig. 1.1(a). However, for an individual with AF, the heart's electrical signals begin in another part of the atria or in the nearby pulmonary veins, instead of SA node. The signals travel throughout the atria in a disorganized way, causing chaotically beating atria and fast beating ventricles. The AF electrical pathways and EKG is shown in Fig. 1.1(b).

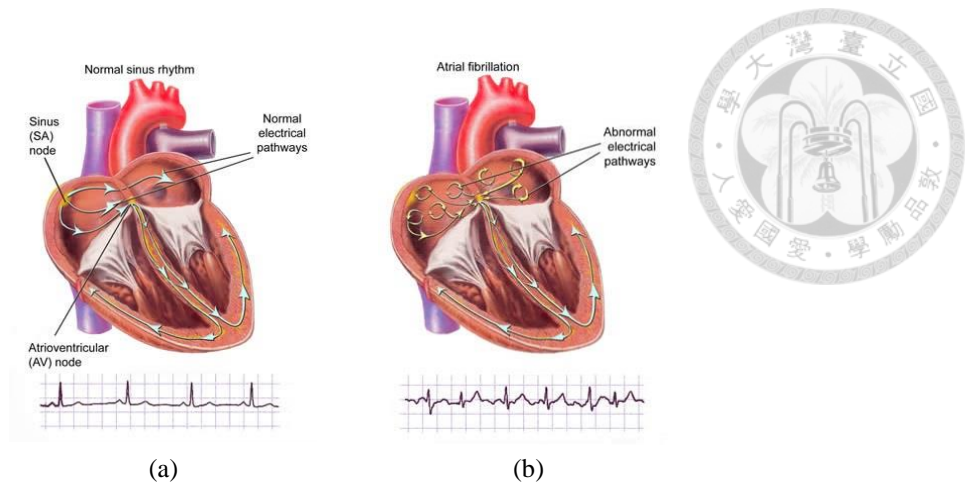


Fig. 1.1 Heart activity of (a) Normal sinus rhythm (NSR), and (b) Atrial fibrillation (AF) [2]

The real danger of AF is the increased risk for stroke. AF is a risk factor for stroke, increasing risk about five-fold [3]. During AF, the atria contract chaotically and in a disorganized manner. Because the atria do not move blood properly, blood pools and gets stuck in the grooves of the heart. This may result in the formation of blood clots, which could get pumped to the brain and result in a stroke [2].

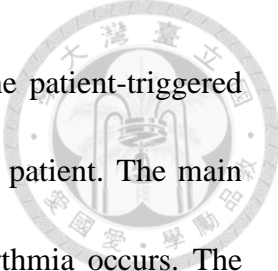
The duration of the AF and underlying reasons for the condition help medical practitioners classify the type of AF problems. By the duration and characteristics of AF, patients can be classified into Paroxysmal AF, Persistent AF and Permanent AF [4]. Paroxysmal AF is when AF occurs only for a period of time and returns to a normal rhythm. Paroxysmal AF is very unpredictable and often can turn into a permanent form of atrial fibrillation. Persistent AF when AF lasts for longer than 48 hours. Permanent AF occurs when the condition lasts indefinitely and can no longer be controlled with medication.



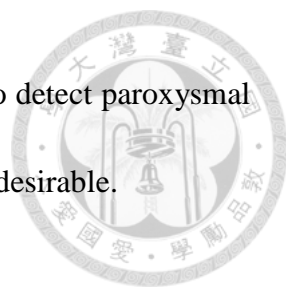
1.1.2 Current diagnosis of AF

The diagnosis of atrial fibrillation involves a determination of the cause of the arrhythmia, and classification of the arrhythmia. Diagnostic investigation of AF typically includes a complete history and physical examination, ECG, transthoracic echocardiogram, complete blood count, and serum thyroid stimulating hormone level [5]. The most common and useful test for diagnosing AF is electrocardiogram (EKG) [1]. As mentioned in Sec.1.1.1, AF occurs if rapid, disorganized electrical signals cause the atria to contract irregularly. Therefore, a typical EKG record shows the absence of P waves, with disorganized electrical activity in their place, and irregular R-R intervals due to irregular conduction of impulses to the ventricles [6]. The short-term EKG diagnosis may failed to detect paroxysmal AF. To detect more potential paroxysmal AF patients, long-term recording of EKG is necessary [7]. Paroxysmal AF can only be precisely detected with long-term monitoring devices.

EKG can be recorded by several cardiac monitoring devices [1], such as the Holter monitoring, the patient-triggered event monitors, mobile cardiovascular telemetry, the patient monitors, and the implantable loop recorder as shown in Fig. 1.2. When one records EKG by a Holter monitor, there are electrodes on the chest and a recording device continuously records the EKG signals around the neck or waist. The usual



duration of the Holter monitoring are 24 to 48 hours [10] [11]. The patient-triggered event recorder records the EKG signals when it is activated by the patient. The main limitation is that the patient should activate the device when arrhythmia occurs. The mobile cardiovascular telemetry allows continuous recording and transmits the arrhythmic EKG signals for remote monitoring [8]. Event recorder and mobile cardiovascular telemetry's usual duration is up to one month, [10] [11]. The implantable loop recorder is implanted device, which can be triggered automatically. Its usual duration is up to two years. Furthermore, implantable loop recorders can transmit the arrhythmic EKG signals to remote monitoring. However, it is costly and invasive compared to the other cardiac monitoring devices. The patient monitors are devices usually attached to the sickbed in intensive care units (ICU). They can monitor and record patients' physiological signals as long as the devices are on. The main drawback is they are for hospitalized patients, therefore not portable and costly. To sum up, each EKG monitoring device has its limitations or drawbacks [10], such as short monitoring period (the Holter monitoring), requiring patients to trigger the recorder (the patient-triggered event recorder), high cost (mobile cardiovascular telemetry and patient monitors), being non portable (patient monitors) or invasive examination (the implantable loop recorder). Furthermore, all EKG monitors requires one lead on each arm. The pros and cons of these cardiac monitors are shown in Table 1-1. The above



shortages make EKG monitors inefficient in long-term monitoring to detect paroxysmal AF patients. Therefore, other tools for AF detection or diagnosis are desirable.

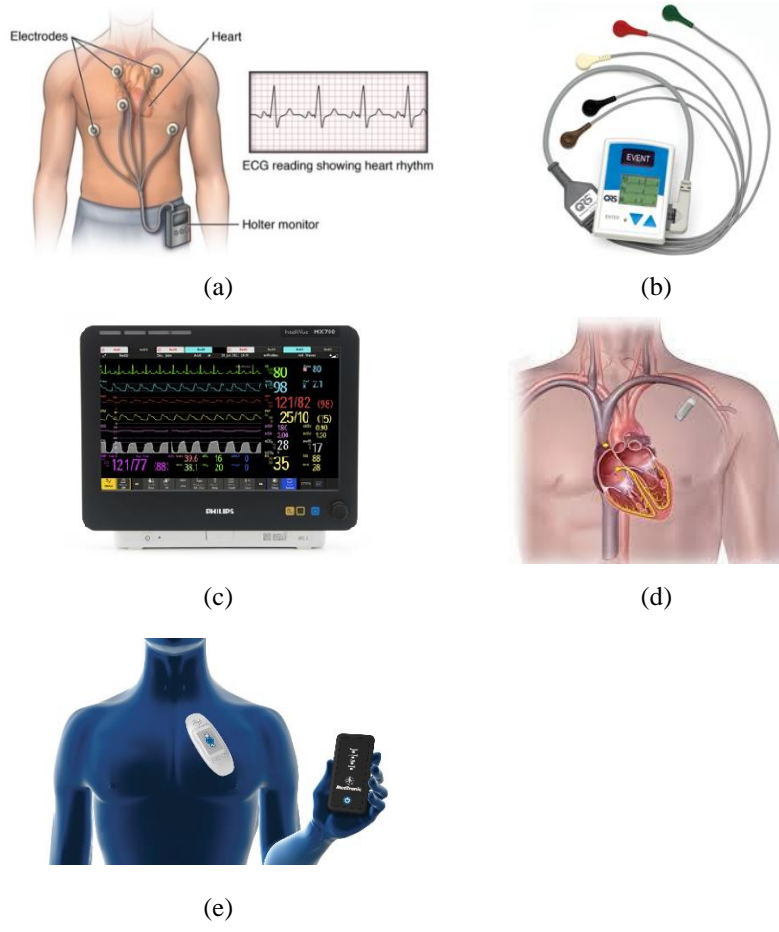


Fig. 1.2 (a) Holter monitoring. (b) Patient-triggered event monitor (c) Patient monitor (d) Implantable loop recorder (e) Mobile cardiovascular telemetry [1] [2] [8] [13]

Table 1-1 The pros and cons of cardiac monitoring devices [8] [10] [11]

Devices	Advantages	Disadvantages
Holter monitoring	<ul style="list-style-type: none"> ● Continuous recording ● Detect asymptomatic events 	<ul style="list-style-type: none"> ● Short monitoring period
Patient-triggered event recorder	<ul style="list-style-type: none"> ● Longer monitoring period ● Correlation of symptoms and rhythm 	<ul style="list-style-type: none"> ● Require patients participation ● Does not detect asymptomatic events
Patient monitors	<ul style="list-style-type: none"> ● Very long monitoring period ● Continuous recording ● Detect asymptomatic events ● Data transmission for remote monitoring 	<ul style="list-style-type: none"> ● Non portable ● Costly
Mobile cardiovascular telemetry	<ul style="list-style-type: none"> ● Longer monitoring period ● Continuous recording ● Detect asymptomatic events 	<ul style="list-style-type: none"> ● Costly
Implantable loop recorder	<ul style="list-style-type: none"> ● Very long monitoring period ● Data transmission for remote monitoring 	<ul style="list-style-type: none"> ● Costly ● Invasive

1.2 Motivation and Contribution of PPG-based AF Detection

In Sec.1.1, it is mentioned that the most common and useful test for diagnosing AF is EKG. However, other tools for long-term monitoring are desirable. On the other hand, photoplethysmogram (PPG) is a technique to obtain the oxygen saturation of blood and heart rate by pulse oximetry. The introduction and motivation of utilizing PPG signals in AF detection will be illustrated in this session.



1.2.1 Introduction of PPG signal

PPG is an electro-optical technique of measuring the cardiovascular pulse wave in the human body [12]. It uses an invisible infra-red light (or red light) emitted into the tissue and the amount of the transmissive or reflective light detected by the photodiode. The measured pulse wave is mainly caused by the periodic pulsations of arterial blood volume, which in turn induces a change in the optical absorption measured. Hence, the periodicity of PPG results from the change of blood volume, which is according to the heart cycle. As a result, the PPG signal is synchronized with heartbeat. The example of a photoplethysmographic waveform is shown in Fig. 1.3.

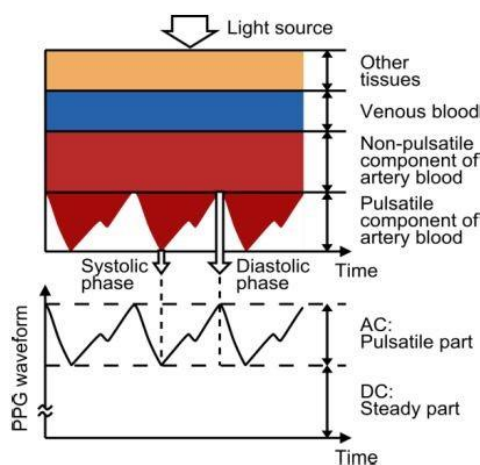


Fig. 1.3 Example of a photoplethysmographic waveform [12]

1.2.2 Motivation and Contribution

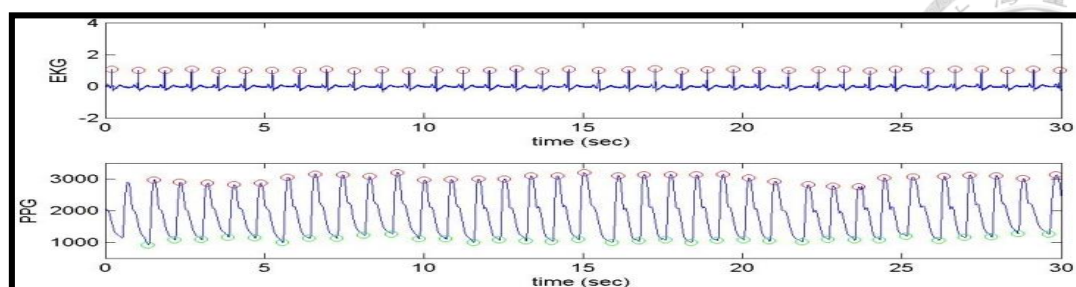
The detection of AF should be long-term for paroxysmal AF. The shortages of

EKG monitors make EKG inefficient in long-term monitoring to detect paroxysmal AF patients. Compared to EKG examination, PPG examination is more convenient and suitable for long-term monitoring. PPG can be measured from comfortable wearable devices such as fingertips, wrists, or earlobes as shown in Fig. 1.4. And PPG sensors require only one lead. The above advantages of PPG signals make PPG a potential tool to assist AF detection.

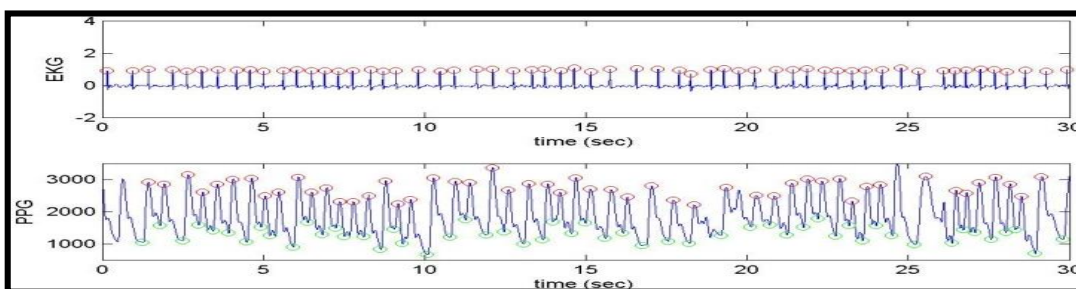
As mentioned in Sec.1.2.1, PPG signal is synchronized with heartbeat along with EKG. Therefore, the characteristics of AF and other kind of arrhythmia may be shown on PPG signals, too. The PPG and EKG signals with normal sinus rhythm (NSR) and AF are recorded from NTUH ICU is shown in Fig. 1.5. From the figure, we find that AF affects PPG signals not only on interval, but also amplitude. Fig. 1.5 has shown the potential of PPG-based AF detection.



Fig. 1.4 PPG devices of (a) Pulse oximetry, and (b) Wrist-type PPG sensor watch [13]



(a)



(b)

Fig. 1.5 PPG and EKG signals with (a) normal sinus rhythm (NSR), and (b) AF

The aim of this thesis is to investigate the potential of analyzing PPG waveforms to identify patients with AF. Furthermore, two clinical scenarios, long-term monitoring and fast screening were considered in the thesis. The PPG-based AF detection framework can be used for long-term monitoring suspected AF patients. The aim of long-term monitoring is to precisely detect paroxysmal AF patient and find the duration of AF to assist doctors' decision of treatment. On the other hand, the framework can be used as a screening tool to assist doctors. The aim of fast-screening is to detect whether an individual has AF with very short recording of signals. For example, screen out the potential AF individuals with only 1 minute of PPG signals. With the predicted outcome and the real diagnosis outcome, accuracy criteria can be calculated using the confusion



matrix, as shown in Fig. 1.6. The importance and need of fast screening and long-term monitoring are mentioned in [7] and [14], respectively. The details of related work will be illustrated in Chapter 2. And the concepts of fast screening and long-term monitoring are shown in Fig. 1.6 and Fig. 1.7, respectively.

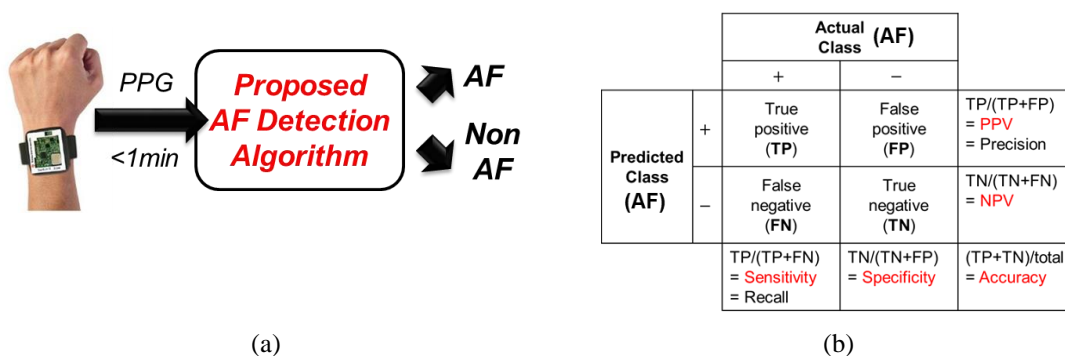


Fig. 1.6 (a) The concept of fast screening AF detection, and (b) Confusion matrix

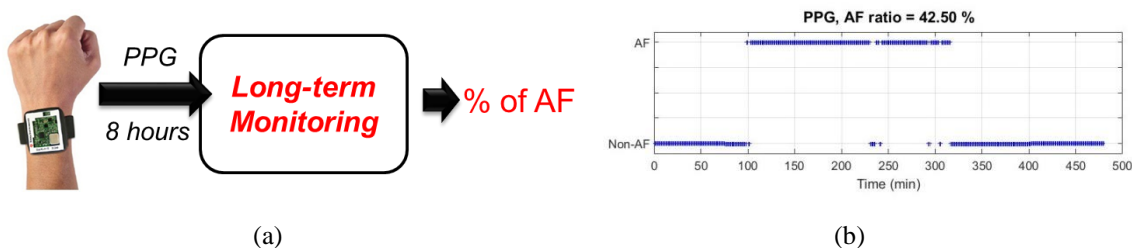
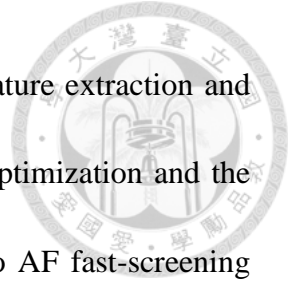


Fig. 1.7 (a) The concept of long-term monitoring AF detection, and (b) An example of long-term monitoring

1.3 Thesis Organization

This thesis is organized into six chapters and shown as follows: In Chapter 2, an overview of automatic AF detection algorithm is given. In addition, some related works of AF detection with EKG and PPG are also introduced. In Chapter 3 and Chapter 4, a

PPG-based AF detection framework is proposed. Preprocessing, feature extraction and the statistical analysis are illustrated in Chapter 3. Classification, optimization and the result are illustrated in Chapter 4. In Chapter 5, the applications to AF fast-screening and long-term monitoring is introduced. Validation on MTK devices and implementation of GUI are also included in Chapter 5. Last, we conclude this thesis and suggest some future directions in Chapter 6.





Chapter 2

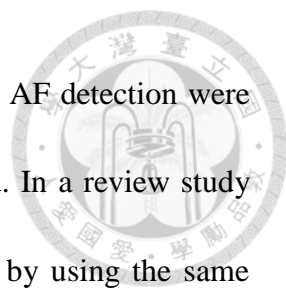
Related Works of AF Detection

In this chapter, we will first introduce the state-of-the-art AF detection algorithms with EKG and PPG. Then we discuss the related works of clinic application of AF detection. Two clinical scenario, fast screening and long-term AF detection will be introduced.

2.1 AF Detection algorithms

2.1.1 EKG-based AF detection

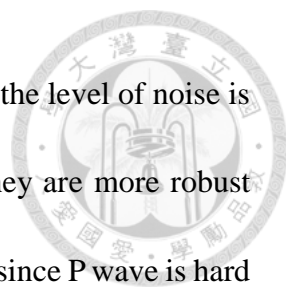
Automatic detection of AF is necessary for the long-term monitoring of patients who are suspected to have AF. State of art methods for EKG-based AF detection are mainly based on two different characteristics of EKG. The irregularity of RR intervals (RRI) and the atrial activity. As mentioned in Sec.1.1, first, during AF, the electrical signals travel throughout the atria in a rapid and disorganized way, ~~causing~~ cause chaotically beating atria and fast beating ventricles. As a result, the RR intervals (RRI) become more irregular and usually fast. Second, electrical atrial activity in atrial is disorganized. The atrial activity is characterized by the absence of the P-wave (PWA) and



special frequency properties (FSA) [15]. The existing algorithms in AF detection were not always evaluated with the same datasets and evaluation method. In a review study [15], several AF detection algorithms were selected and evaluated by using the same method and MITBIH Arrhythmia Database. The related works can be classified into RR intervals (RRI) based, atrial activity (AA) based and combination of RRI and AA

The R wave is the most detectable and distinctive characteristic in EKG waveforms. Therefore, the RRI-based related work are the major part of the related researches. Related algorithms in [15] including using a simple variance feature, a statistical framework combination, Kolmogorov Smirnov test and regressive modeling. On the other hand, P wave is the most relevant characteristic to AF. Time domain AA analysis consists of detecting the P wave or finding the P wave absence. Frequency spectrum AA analysis requires cancellation of ventricular activity (QRS complex and T wave) and Fourier analysis of the remaining P wave. Some researches combine RRI and AA algorithms to enhance the performance. Among all the related works referenced in [15], [16] performs the lowest error rate and is the only framework with 90% performance in all accuracy criteria. It is worthwhile to mention that, in [16], only traditional standard RRI histograms and Kolmogorov Smirnov test were used to separate AF and non AF RRI histograms.

In conclusion, the traditional RRI-based related work shows the best performance



in review studies. The reason may be that, in ambulatory conditions, the level of noise is high and therefore, the algorithms based on RRI are preferred as they are more robust against noise [15]. By contrast, AA-based algorithms perform poorly since P wave is hard to detect when the noise level increases.

2.1.2 PPG-based AF detection

Contrary to the amount of EKG-based AF detection related works, there are few PPG-based AF detection related works. The main PPG-based related works with open algorithms are [17], [18], [19] and [20]. These studies were published by the same group of authors, in 2012 EE conference, 2013 EE journal, 2013 medical journal, and 2015 EE journal, respectively. In these studies, AF detection using the PPG signals measured from iPhone cameras is demonstrated, as shown in Fig. 2.1. In these studies, the measurement time for each subject is about 2 to 5 minutes. Data collection consists of two stages by cardioversion, which makes arrhythmia patients' waveforms return to normal for a short period of time. The first stage is the pre-electrical cardioversion, and the PPG signals measured from AF patients are regarded as AF. The second stage is the post-electrical cardioversion, and the PPG signals measured in this stage are regarded as normal sinus rhythm (NSR).



Fig. 2.1 iPhone 4S prototype for AF detection [18]

In the training phase, the EKG signals in MIT-BIH AF database and MIT-BIH NSR database are used to build the models. First, the parameter, the R-R interval (RR), is extracted from the EKG signals. Second, selected features, including normalized root mean square successive difference between adjacent data points (normalized RMSSD), Shannon entropy (ShEn), and sample entropy (SampEn) were extracted from RRI. The models were built by finding the threshold values of the features that provided the largest area under the receiver operating characteristic (ROC) curves in binary classification of AF and NSR. In the testing phase, the PPG signals measured by the studies were used to test their models. First, the parameter, the pulse-pulse interval (PPI), was extracted from the PPG signal. Second, the same features from the training phase, were extracted from interval series. Then, these features were used to test the models. The testing flow chart is shown in Fig. 2.2. They achieved high accuracy in prediction and proved that PPG-based AF detection is a promising tool. The comparisons of performances of the PPG-based AF detection are summarized in Table 2-1.

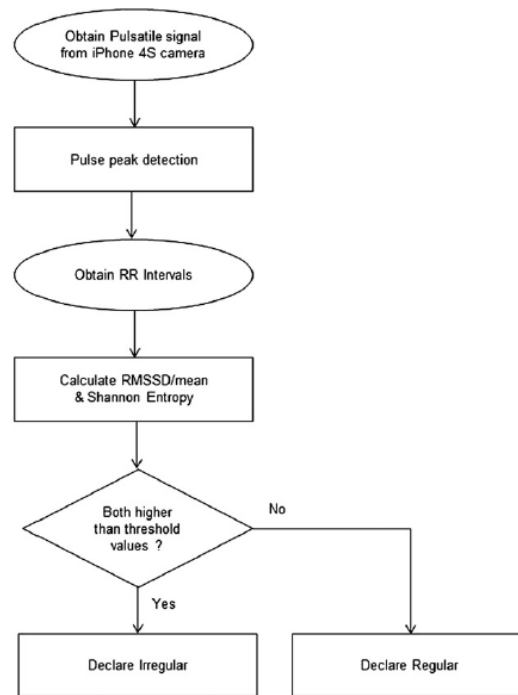
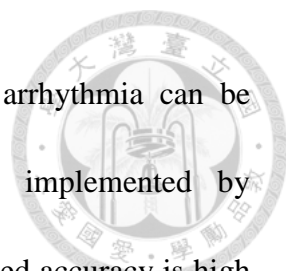


Fig. 2.2 The flow chart of testing [19]

Table 2-1 The comparisons of performances in related works [17] [18] [19] [20]

	Subjects	Features	Accuracy	Sensitivity	Specificity
Jinseok <i>et al.</i> [17][18]	25	Normalized RMSSD	98.44	97.63	99.61
		ShEn	89.94	74.61	100.0
		SampEn	95.52	92.58	99.80
		All 3 features	99.51	---	---
McManus <i>et al.</i> [19]	76	Normalized RMSSD	95.33	98.18	91.50
		ShEn	90.97	97.50	82.18
		All 2 features	96.76	96.19	97.52
Jo Woon Chong <i>et al.</i> [20]	99	Normalized RMSSD ShEn TPR	96.26	---	---

In [20], other types of arrhythmia have been considered, too. Subjects with AF, PVCs and PACs can be distinguished from each other. First, the arrhythmia waveforms are separated from NSR. Then, Poincare plot is used to separate AF, PVCs and PACs by



RRI's turning pattern. This work further prove the potential of arrhythmia can be detected by PPG signals. Moreover, the framework can be implemented by cost-effective and standard devices such as smart phones. The claimed accuracy is high and the smart phone based implementation is impressive. However, these studies have the following limitations in experiment settings and algorithms, which may make them overestimate the accuracy of their framework:

1. The sample size is small. And the experiment data are collected in standardized environments. Therefore, it is possible that real clinic interference like baseline or other diseases might influence the performances of the PPG-based AF detection [19].
2. The training and testing data are based on EKG and PPG, respectively. The experiment is based on the hypothesis that EKG's R-R interval (RRI) is the same as PPG's pulse interval (PPI).
3. And NSR data are not all collected by NSR individual. The PPG signals measured after cardioversion are regarded as normal sinus rhythm (NSR). The experiment is based on the hypothesis that the signals after cardioversion are always the same as NSR individual.
4. The framework lacks baseline preprocessing.



5. The framework only takes one of the PPG parameters, the pulse interval (PPI), into consideration.
6. The framework lacks feature variety.
7. The framework only apply basic classification algorithm, such as selecting a threshold for best accuracy.
8. The framework cannot support fast screening and long-term monitoring.

All these drawbacks will be improved in the proposed framework, which will be introduced in Chapter 3 and Chapter 4.

2.2 AF Detection Application: Fast-screening and Long-term Monitoring

2.2.1 Long-term monitoring AF detection

Paroxysmal AF can be a risk factor for ischemic stroke or transient ischemic attack (TIA) patients because it is asymptomatic and undetected by traditional monitoring techniques. In [7], 572 patients with stroke or transient ischemic attack (TIA) are randomly separated into two different groups. One group of patients are monitored in long-term by 30-day event-triggered loop recorder. The other group of patient are monitored in short-term by conventional 24-hour Holter monitor. The number of

subjects detected AF by long-term monitoring is 5 times higher than by Holter monitor.

In addition, when the duration of EKG monitoring is prolonged, the number of detected AF also increases, as shown in Fig. 2.3. As a result, the study concludes that long-term EKG monitoring significantly improves the AF detection compared with the short-term EKG monitoring. Many medical researches with similar conclusion were summarized in the review journal [21]. To sum up, long-term monitoring for AF detection achieve higher detect rate of AF and is necessary in detecting paroxysmal AF.

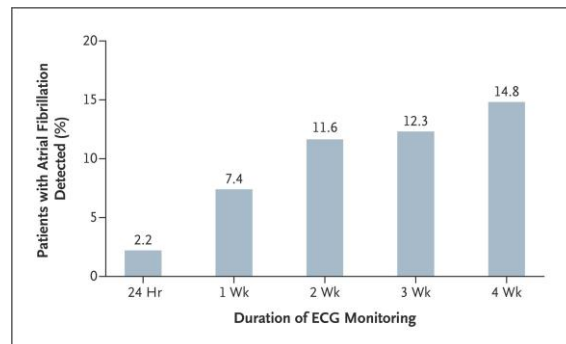


Fig. 2.3 The percentage of detected AF when the duration of EKG monitoring is prolonged [7]

2.2.2 Fast screening AF detection

Diagnosing AF before ischemic stroke occurs is a priority for stroke prevention in AF. As mentioned in Sec.2.1.2, PPG-based AF detection is done using smartphone [17] [18] [19] [20], however, its ability to diagnose AF in real-world situations has not been adequately investigated until a recent research [14] published. In [14], the diagnostic performance of a standalone smartphone PPG application, Cardio Rhythm, for AF



screening in primary care setting is investigated. Patients with hypertension, with diabetes mellitus, and/or aged ≥ 65 years were recruited. EKG was recorded by using the AliveCor heart monitor and AF detector [23]. And the waveforms were reviewed by 2 cardiologists to provide the reference standard.

PPG measurements were performed by using the Cardiio Rhythm smartphone application, of which algorithm was patented in [22]. Patients were instructed to place the tip of their index finger of either hand on the camera of the iPhone, as shown in Fig. 2.4. Each PPG waveform recording lasted only 17.1 seconds and was classified automatically by the Cardiio Rhythm smartphone application as “Regular” or “Irregular”. Finally, the outcome was compared to the reference diagnosis by 2 cardiologists reviewing the EKG signals. And the automatic classification result of AliveCor heart monitor was also compared. The performance of AliveCor heart monitor and Cardiio Rhythm smartphone application is compared in this work. The result is summarized in Table 2-2.

Table 2-2 Summary of performance comparisons [14]

	Sensitivity	Specificity	PPV	NPV	Record Time
Cardiio Rhythm application	92.9 %	97.7 %	53.1 %	99.8 %	17 Seconds
AliveCor heart monitor	71.4 %	99.4 %	76.9 %	99.2 %	30 Seconds

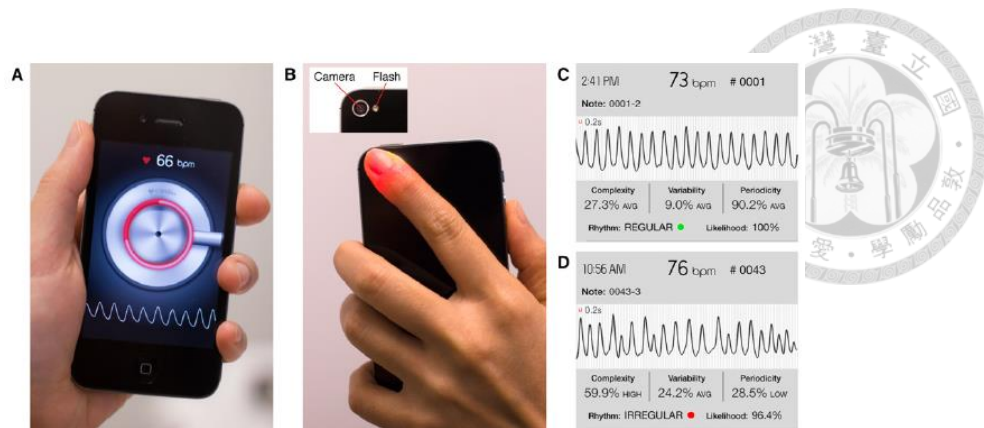


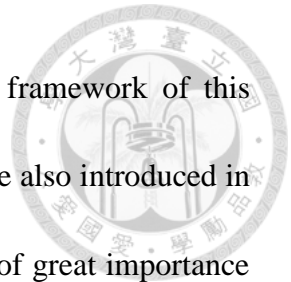
Fig. 2.4 Smartphone camera-based PPG measurements (A) The Cardio Rhythm standalone smartphone application. (B) Example of measurement. (C) Examples of PPG recordings from normal sinus rhythm. (D) Examples of PPG recordings from an AF patient [14]

As a result, the study concludes that The Cardio Rhythm smartphone PPG application is able to detect AF with a high accuracy and comparable to the EKG-based AliveCor automated AF detector. Moreover, its application is as a screening tool, and not as a substitute for the standard EKG and doctor diagnosis. For a screening test, it is important to have a high sensitivity. The potential subjects should be further diagnosed by cardiologists with EKG recording. To sum up, fast screening for AF detection can assist cardiologists screen out the potential AF patients in very short period of recording. The PPG-based AF screening application is both cost and time effective and broad accessible.

2.3 Summary

In this chapter, some related works of AF detection algorithm with EKG and PPG are introduced. However, there are some limitations and drawbacks in the related works.

These drawbacks in algorithm will be improved in the proposed framework of this thesis. Long-term and fast screening AF detection medical studies are also introduced in this chapter. Since the consideration of the two clinical scenarios is of great importance when it comes to real clinical use. The two clinical scenarios, long-term monitoring and fast screening are considered as the intended application of the proposed framework.





Chapter 3

Pre-processing and Feature Extraction of PPG-based AF Detection

In this chapter, we will first introduced the flowchart of the proposed framework. And the signal processing part of the proposed framework, including pre-processing, baseline removal and feature extraction will introduced. The result of statistical analysis of features is shown in the end of this chapter.

3.1 PPG-based AF Detection Framework

The flowchart of related work [20] is shown in Fig. 3.1. As mentioned in Sec.2.1.2, there is still performance gap between related works and EKG-based algorithm. In addition, the PPG-based AF detection related works have the following limitations in algorithm:

1. The framework lacks baseline preprocessing.
2. The framework only takes one of the PPG parameters, the pulse-pulse interval (PPI), into consideration. However, in Sec.1.2.2, we find that AF affects PPG signals



not only interval, but also amplitude.

3. The framework lacks feature variety.

4. The framework only apply basic classification algorithm, such as selecting a threshold for best accuracy.

5. The framework did not investigate different data length of input signals. Therefore, it cannot support long-term monitoring and fast screening.

All these drawbacks will be improved in the proposed framework. Therefore, a PPG-based AF detection framework is proposed, the proposed and enhanced flowchart is shown in Fig. 3.2. The comparisons with related works are summarized in Table 3-1. The signal processing part of the proposed framework, including data collection, pre-processing, baseline removal and feature extraction will introduced in Chapter 3. While the learning part, including feature selection and classification will introduced in Chapter 4. The details of signal processing part will be illustrated successively in the following sections.

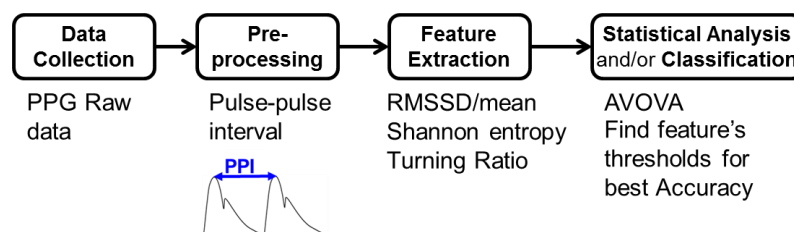


Fig. 3.1 The flowchart of related work [20]

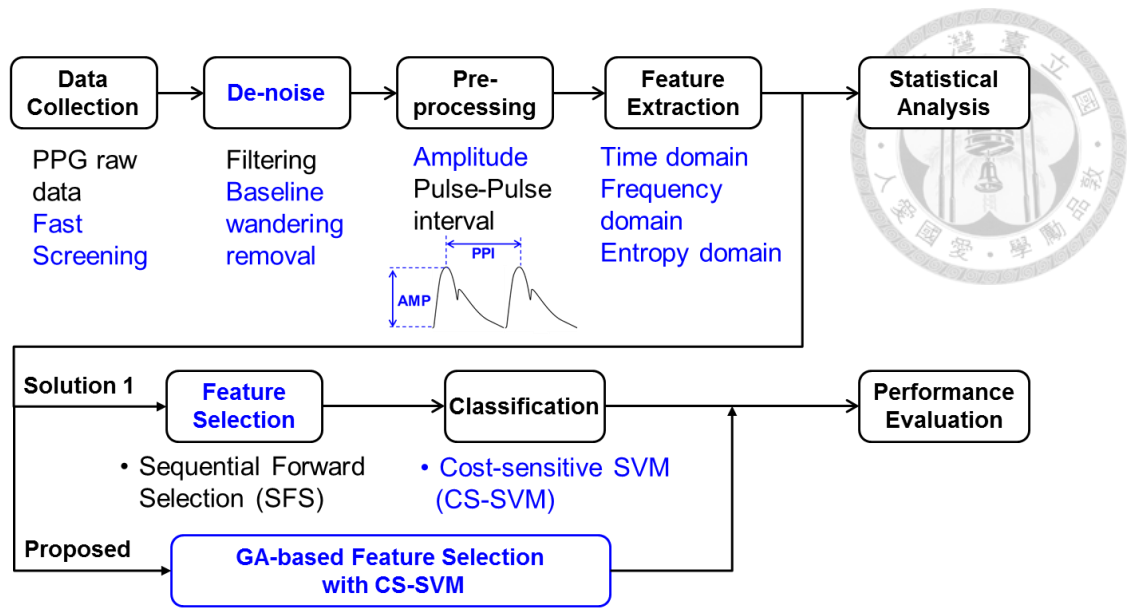


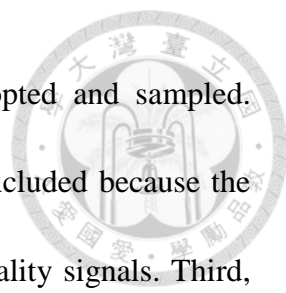
Fig. 3.2 The flowchart of the proposed framework

Table 3-1 Comparisons of related work and proposed frameworks

	Jointly Analysis of Parameters	Variety of Features	Feature Selection	Classification Algorithms	Fast Screening
Related work [20]	No	3	No	Basic	No
Proposed Framework	Yes	56	Yes	CS-SVM	Yes

3.2 Data Collection

The experiment data are from the intensive care unit (ICU) of stroke in National Taiwan University Hospital. The data was collected from February, 2012 to Nov, 2015. The EKG and PPG signals were recorded synchronously by patient monitors with sampling frequency 512 Hz and 128 Hz, respectively. The total number of the collected patients in this experiment is 803.



First, the first ten-minute signals of each patient were adopted and sampled. Second, the segments without 40 to 150 pulses per minute were excluded because the ones with extreme abnormal heartrate are usually noisy or poor quality signals. Third, each minute EKG is individually labeled as AF, non-AF, or poor signal quality by Dr. Tang and Dr. Hung. The poor quality signals and few signals with both AF and non AF in ten minutes are removed. The label remained the same in ten minute. Finally, after EKG were labeled by doctors, the PPG signals were used for the input of our framework. Moreover, to compare the performance of both PPG and EKG examination, the EKG-based AF detection framework is applied in the same way. The valid number of the collected patients is 673. Among these 673 patients, 151 patients were labeled as AF. Therefore, the AF ratio in this database is 22.4%.

Fast screening is considered in the framework. The fast screening experiment is conducted by manipulating the data length used in the data collection part. PPG signals are vulnerable to noise. Therefore, the screening record time should be shorter for convenience. However, most entropy domain features require enough data length to be calculated. In conclusion, the data length issue in fast screening is a trade-off between accuracy and convenience. To find the shortest data length, we experimented with different data length in the data collection. The experiment will be introduced in Sec.5.1. In this thesis, the data length is 2 minutes unless otherwise stated.



3.3 Pre-processing with Baseline Removal

3.3.1 Baseline wandering in PPG signals and its effects on AF detection

The purpose of pre-processing is to extract parameters from PPG. Most PPG-based AF detection related works focus on using pulse-pulse interval (PPI), which is highly correlated to EKG's RRI. However, we found that PPG's AMP is also affected by AF. The new parameter, PPG's AMP may provide different information other than RRI and increases the accuracy of classification. The idea of utilizing amplitude as a parameter is even rarely seen in EKG-based algorithms, as illustrated in Fig. 3.3.

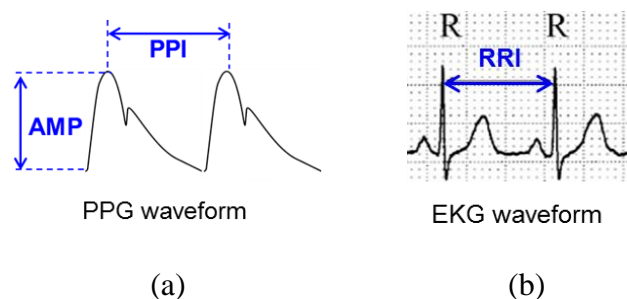
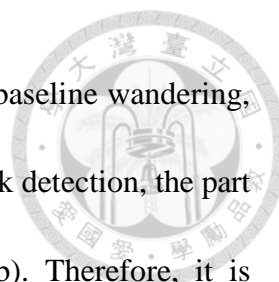


Fig. 3.3 Extracted parameters of (a) PPG, and (b) EKG

Traditionally, the old-school Pan-Tompkins peak detection algorithm [24] and “derivative and threshold” algorithm [25] were used to find the peaks of EKG and PPG signals, respectively. Amplitude (AMP), and pulse-pulse interval (PPI) were extracted from PPG signals. And R-R intervals were extracted from EKG signals for comparison



as well. However, some ICU data and the data from MT2511 have baseline wandering, as shown in Fig. 3.4(a). If the traditional algorithm is applied for peak detection, the part with critical baseline wandering will fail, as shown in Fig. 3.4(b). Therefore, it is necessary to remove the effect of baseline to detect all peaks in PPG signals.

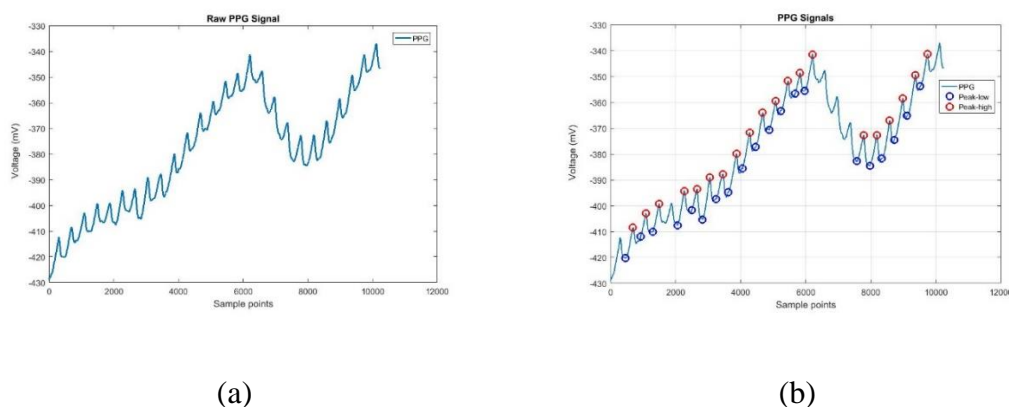


Fig. 3.4 PPG waveforms and the effect of baseline

3.3.2 State-of-the-art baseline removal algorithms

Only PPI and AMP series are needed in AF detection framework, therefore, the original wave form is not key to the accuracy in this work. Since PPI and AMP series should be extracted, the desired baseline removal methods are limited in time domain de-noising. The state-of-the-art time domain baseline wandering removal algorithms [26] [27] are introduced:

1. PCA-based algorithms: PCA-based algorithms usually require periodic signals [28]



[30]. Since AF physiological signals contain time variant noise and non-stationary trends, PCA-based algorithms are not suitable for this framework.

2. Adaptive filters: Reference signals such as accelerator signals or respiratory signals are need for adaptive filtering de-noising [29]. Adaptive filters cannot be applied because the lack of reference signals.

3. Band pass filters: Band pass filters are easy to design and frequently used. The PPG signals' frequency range is usually 0.5Hz~4Hz [26]. However, it's hard to find an appropriate frequency range to meet everyone's physiological characteristic. And the FIR filter order can be high to meet the narrow band requirement. A band pass FIR filter with range from 0.5Hz to 4Hz and 40dB stopband attenuation is applied to the waveform in Fig. 3.4. The result is shown in Fig. 3.5. The peak can be detected, however, the main drawback is it is hard to find an appropriate frequency range to meet everyone's characteristic and the latency due to high order the of FIR filter.

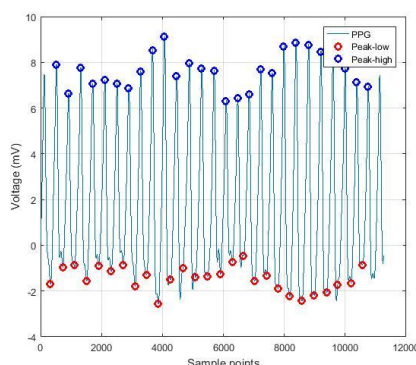
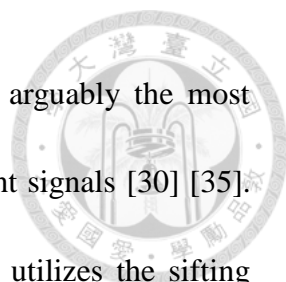


Fig. 3.5 The waveform processed by the FIR filter



4. Ensemble Empirical Mode Decomposition (EEMD): EEMD is arguably the most famous and accurate way to find the baseline or trend in time variant signals [30] [35]. However, the drawback is the high complexity of EEMD. EEMD utilizes the sifting process to iteratively decompose the signal into a set of intrinsic mode functions (IMFs) and a residual shown in Fig. 3.6. In the demonstration, PPG is decomposed into 7 IMFs and 1 residual. EEMD is applied to the waveform in Fig. 3.4. The result is shown in Fig. 3.7. The peak can be detected yet the main drawback is high complexity.

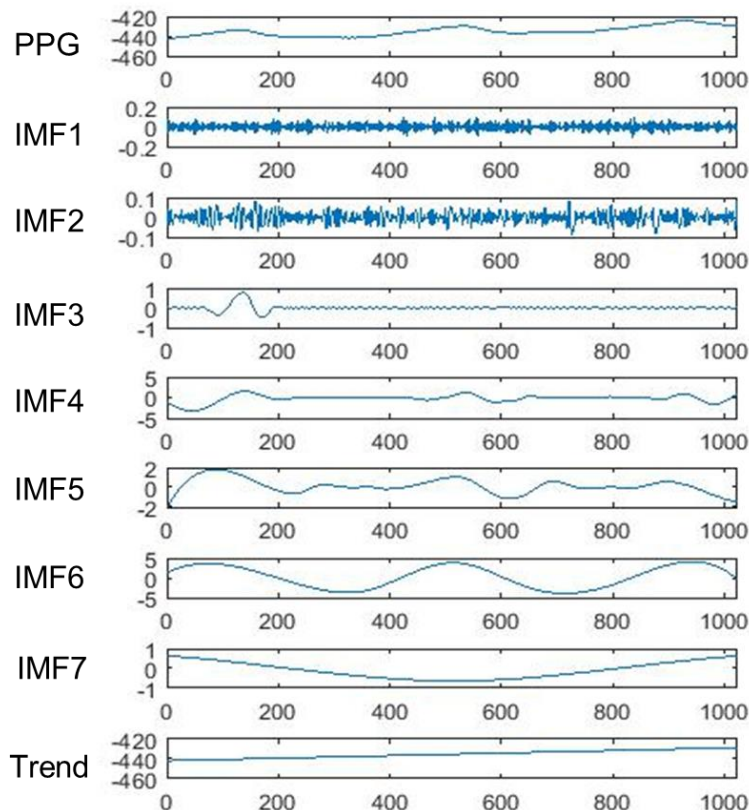


Fig. 3.6 PPG de-trend using empirical mode decomposition

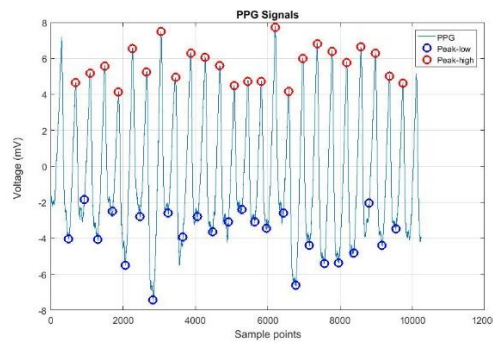


Fig. 3.7 The waveform processed by the EEMD

5. Mathematical Morphological filters (MMF): MMF was usually used in 2D signal processing, such as finger-print processing. Morphological filters modify the shape of a signal by transforming it through its intersection with another object called the structuring element. The basic operators and concepts are shown in Fig. 3.8.

$$\text{Erosion: } A \ominus B \quad (3.1.a)$$

$$\text{Dilation: } A \oplus B \quad (3.1.b)$$

$$\text{Opening: } A \circ B = (A \ominus B) \oplus B \quad (3.1.c)$$

$$\text{Closing: } A \bullet B = (A \oplus B) \ominus B \quad (3.1.d)$$

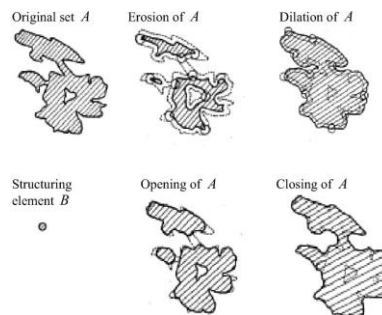
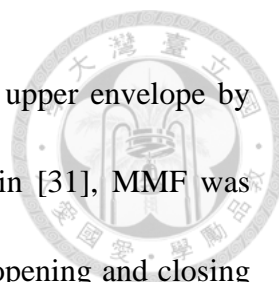


Fig. 3.8 The basic operators of MMF [32]



In 1D signal processing, MMF can be applied to extract the upper envelope by closing and lower envelope (baseline) by opening. For example, in [31], MMF was applied to extract the baseline of EKG signals. The author applied opening and closing on EKG to cancel the baseline, Q wave and R wave pit, with a fixed length flat structure element in [31]. MMF is applied to the waveform in Fig. 3.4. The result is shown in Fig. 3.9(a). The main drawback is the AMP series being deteriorated by MMF, as shown in Fig. 3.9(b).

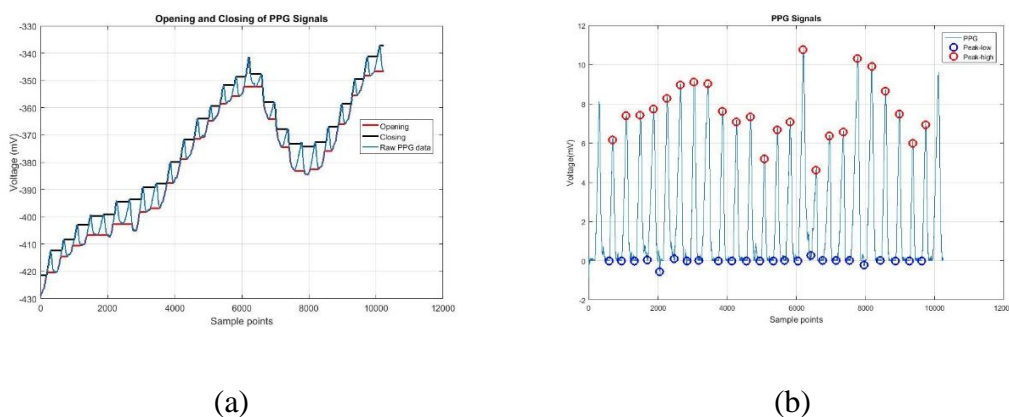


Fig. 3.9 Applying MMF to PPG signals

3.3.3 Proposed MMF-based Pre-processing

Since MMF has the advantage of being adaptive to the time variant signals, low complexity and ability to meet everyone's physiological characteristic. The proposed pre-processing is based on the MMF, and able to overcome the problem that AMP series being deteriorated. The flowchart of the proposed pre-processing is shown in Fig. 3.10.

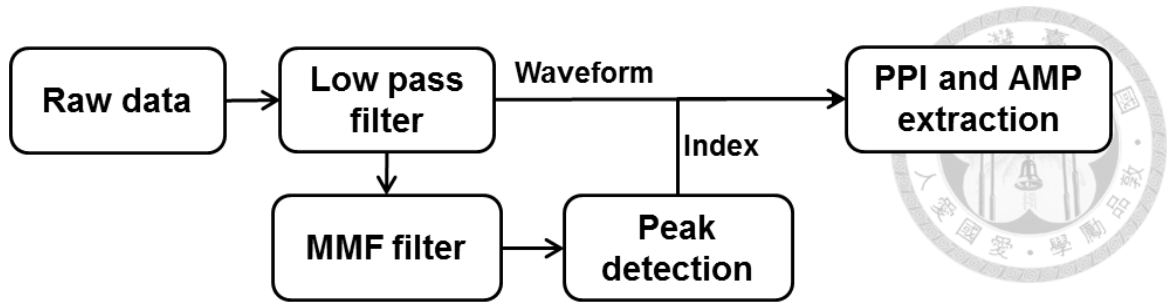


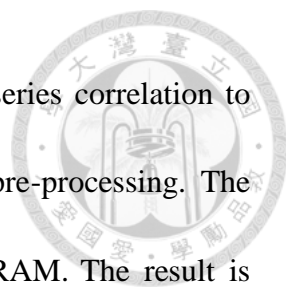
Fig. 3.10 The flowchart of the proposed pre-processing

First, the PPG signals don't have pits like EKG's P wave and T wave. The opening operator is enough to find the baseline. And the structure element S_E is a flat element adaptive to the average heartbeat of the PPG signals. The baseline is extracted to find the MMF filtered signal $f_{signals}$.

$$f_b = f \circ S_E, f_{signals} = f - f_b \quad (3.2)$$

The MMF filtered signal can detect the peak index accurately, though deteriorate AMP. We can find the AMP on the original waveform f with the index found in MMF filtered signal $f_{signals}$. Furthermore, the definition of AMP is modified in the proposed pre-processing. The amplitude of baseline wandering signal can be different in the same pulse, as shown in Fig. 3.11(a). The problem is solved by defining AMP as the average of left and right side amplitude, as shown in Fig. 3.11(b).

To compare the performance of EEMD and MMF, we applied these methods on a segment of 10 minute PPG signals. The EEMD is considered as the reference solution.



The performance can be evaluate by the extracted PPI and AMP series correlation to EEMD's solution. And complexity is evaluated by the time for pre-processing. The equipments of computer are i-7-2600 CPU@ 3.40GHz and 14GB RAM. The result is shown in Table 3-2.

. The result suggests that the proposed MMF based pre-processing can detect the AMP and PPI series reasonably accurate with low complexity.

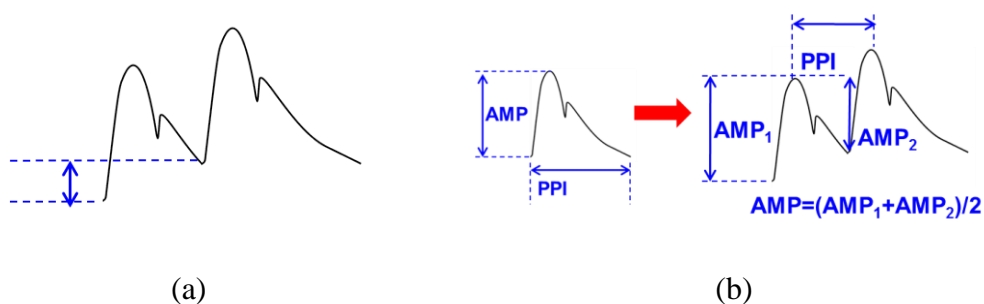


Fig. 3.11 (a) The amplitude of baseline wandering signal, and (b) Modified definition of AMP

Table 3-2 Performance comparisons of pre-processing

	EEMD	Proposed Method
Peak detected	973/973	973/973
PPI correlation	--	0.999
AMP correlation	--	0.998
Time (100 average)	39.5 Secs	0.171 Secs



3.4 Feature Extraction

Time domain, frequency domain and entropy domain features are extracted **from** **the PPI and AMP series, not from raw data**. Except common linear features, three entropy domain features, including multiscale entropy, Shannon entropy and turning point ratio, are applied. The details of each feature are illustrated as follows.

3.4.1 Time domain and frequency domain features

We used some of the most popular linear features in heart rate variety (HRV) researches, according to reference book [33]. Linear features includes time domain features and frequency domain features. Time-domain analysis measures the variation in heart rate over time or the intervals between successive normal cardiac cycles. Mean and standard deviation (SD) represent overall distribution. Root mean square successive difference (RMSSD) is based on interval differences:

$$RMSSD = \sqrt{\frac{1}{N} \sum_{i=1}^N (x_i - x_{i-1})^2} \quad (3.3)$$

Utilizing both SD and RMSSD, the features contain both short-term and long-term variations. Furthermore, to balance the variation in mean value, normalized SD and

normalized RMSSD is calculated by dividing mean value. NN counts ratio (pNNR) is modified from the common HRV feature, pNN50. NN50 is the number of pairs of successive NNs that differ by more than 50 ms. pNN50 is the proportion of NN50 divided by total number of NNs and is thought to show cardiac parasympathetic activity. Because PPG-AMP series are not based on NNs or RRIs, the definition is modified. For example, pNNR(1.1) is the proportion of the number of pairs of successive NNs that has bigger ratio than 1.1 divided by total number of NNs. We choose the ratio thresholds as 1.1, 1.3 and 1.5.

$$pNNR11 = \frac{N\left(\frac{RRI_{i+1}}{RRI_i} > 1.1\right)}{N} \quad (3.4)$$

Frequency-domain analysis describes the periodic oscillations of the heart rate signal. The signals are decomposed at different frequencies and amplitudes, providing information of relative intensity in the rhythm of the heart. Related studies have found that frequency features are related to sympathetic and para-sympathetic nervous systems. We use FFT-based method and calculated the power in low-frequency (LF), power in high-frequency (HF) and LF/HF according to the definition in HRV researches, as shown in Fig. 3.12.

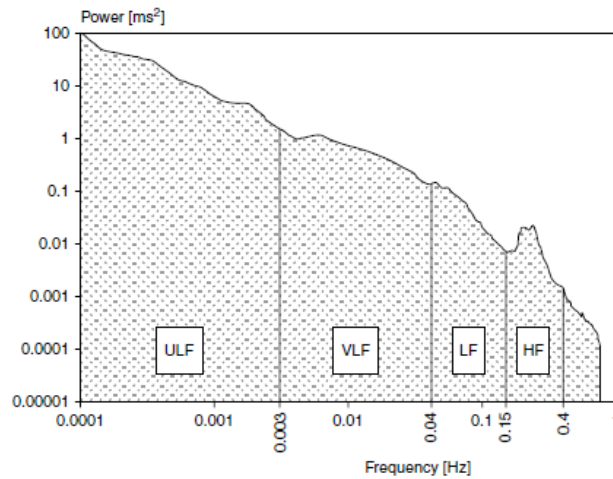


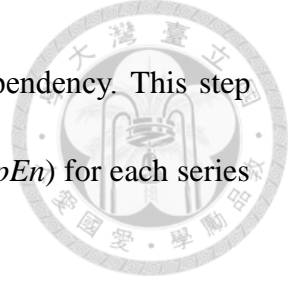
Fig. 3.12 HRV power spectrum over 24 hours [33]

3.4.2 Entropy domain features

1. Multiscale entropy (MSE) [34]: MSE is a non-linear method which has been widely used to evaluate the physiologic control mechanisms, such as heart failure and Alzheimer's disease [35]. In the case of AF detection, AF subjects have more unstable heartbeat, and thus prone to present higher entropy value. There are two steps in MSE. First, the multiple coarse-grained time series are calculated by averaging a successively increasing number of data points in non-overlapping windows:

$$y^\tau = \frac{1}{\tau} \sum_{i=(j-1)\tau+1}^{j\tau} x_i, 1 \leq i \leq N, 1 \leq j \leq \frac{N}{\tau}, \quad (3.5)$$

where x_i is the original time series, N is the length of x_i , and τ is the scale factor. In 2 minutes of PPG signal, we do not have enough pulses to calculate high scale MSE.

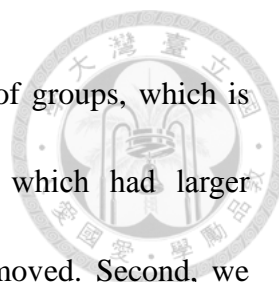


Therefore, τ is set to be 3 due to sample entropy's data length dependency. This step generates different time series y^τ . Second, the sample entropy (*SampEn*) for each series y^τ is calculated as:

$$SampEn = -\ln \left[\frac{B^{m+1}(r)}{B^m(r)} \right], \quad (3.6)$$

where m is the pattern length and r is the similarity criterion. $B^m(r)$ is the number of two sets of simultaneous data points of length m have distance $< r$. And we set $m=2$ and $r = 0.2$ in the experiment. *SampEn* is the conditional probability that a dataset, having repeated itself within a tolerance r for m points, will also repeat itself for $m + 1$ points. The more complex the signal is, the higher the entropy value will be.

2. Shannon entropy (*E_Shannon*): Shannon entropy is a common entropy definition in information theory. Shannon's measure of information is the probability of symbols to represent the amount of uncertainty or randomness of data. However, how to define parameter series into symbols can be flexible. Distribution of parameters differs a lot among patients, therefore, fixing thresholds between symbols is inappropriate. If we use fixed thresholds to calculate Shannon entropy, the box plot of AF and non-AF is shown in Fig. 3.13(a). The p-value is 0.18, which is larger than 0.05. The result suggest no statistical significance.



Therefore, we classify parameter series into a fixed number of groups, which is closer to Shannon entropy's original definition. First, outliers, which had larger difference to mean value than three standard deviations, were removed. Second, we sorted rest data into equally spaced N bins, where N is the number of bins. Last, we calculate the probability p_i of each bins and apply Shannon entropy:

$$E_{shannon} = - \sum_{i=1}^N p_i \log(p_i). \quad (3.7)$$

The optimal number of groups is data dependent, therefore, we applied $N = 4, 8, 16, 32$ and 64 for experiment. We find the modified Shannon entropy has better statistical significance with p value $< 10^{-10}$. The boxplot is shown in Fig. 3.13(b).

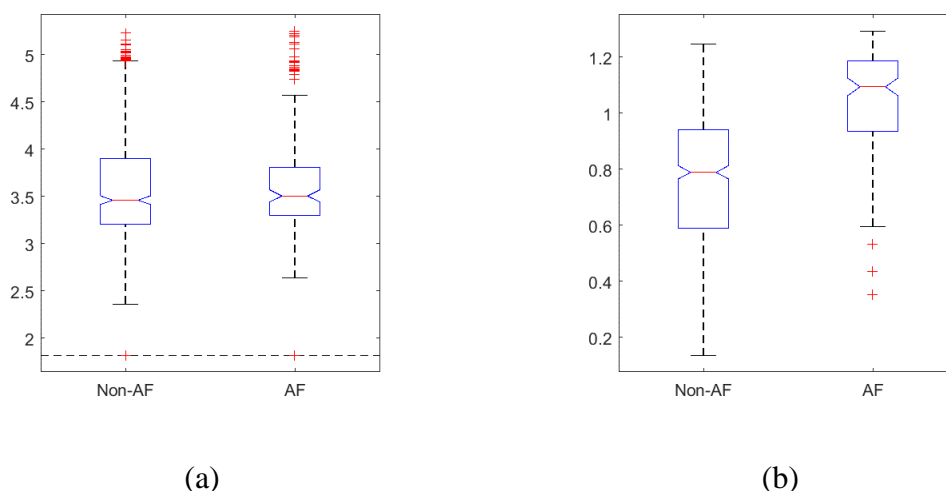


Fig. 3.13 The boxplot of (a) Shannon entropy calculated by fixed threshold, and (b) Modified Shannon entropy calculated by fixed group number



3. Turning point ratio (TPR): TPR is proposed based on the nonparametric “Runs Test” to measure the randomness in a time-series [36], and the idea is used in EKG-RRI [37]. Each beat in a RRI series is compared to its two nearest neighbors and is defined a turning point if it is greater or less than two neighbors. TPR is the ratio of turning point to total data length L. TPR is higher when series is more random.

$$TPR = \frac{RRI_i | (RRI_i - RRI_{i-1})(RRI_i - RRI_{i+1}) > 0}{L}. \quad (3.8)$$

And TPR is applied on PPG parameters in the same way. Furthermore, we also extracted the trend of series and then perform TPR to build the modified version of TPR (TPR2). The purpose is to find the turning point of the trend of series, which is different from the original definition. They both have good statistical significance with p value < 10^{-10} , as shown in Fig. 3.14. For each parameter, we extract all these features as candidate features. All candidate features are listed in Table 3-3 .

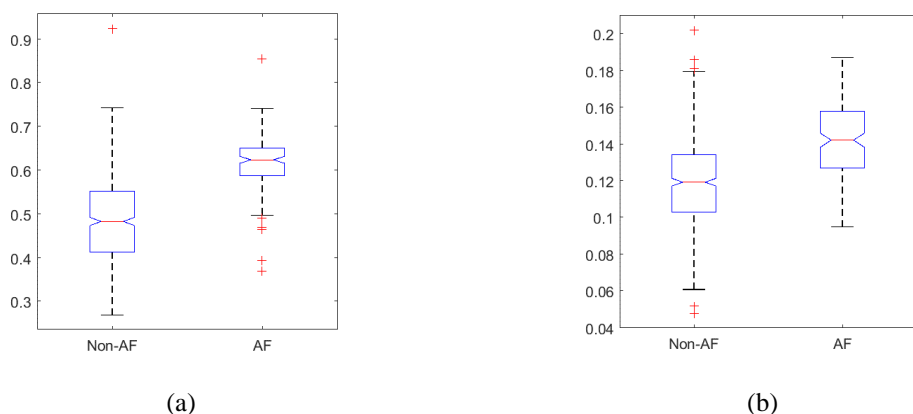


Fig. 3.14 The boxplot of (a) TPR1, and (b) TPR2



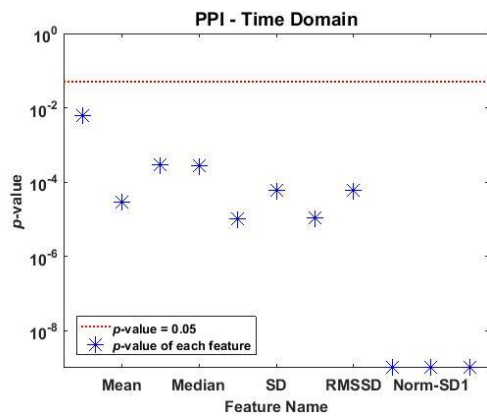
Table 3-3 All candidate features

Extracted Feature	Physiological Meaning	N
Mean value (<i>Mean</i>) , Median value (<i>Median</i>)	Average and median	2
NN counts ratio (<i>pNNR(ratio)</i>) Ratio: 1.1, 1.3, 1.5	Successive ratio of parameter	3
Standard deviation (<i>SD</i>), Normalized SD	Long-term variability	3
Root mean square successive difference (<i>RMSSD</i>), Normalized RMSSD	Short-term variability	3
Power in very low-frequency range 0.003-0.04 Hz (<i>VLF</i>)	Low frequency term	1
Power in low-frequency range 0.04-0.15 Hz, (<i>LF</i>) , Normalized LF	Sympathetic nervous systems: tensioned	2
Power in high-frequency range 0.15-0.4 Hz, (<i>HF</i>) , Normalized HF	Parasympathetic nervous systems: relaxed	2
Ratio of power in low-frequency range and power in high-frequency range (<i>LF/HF</i>)	Balance between the sympathetic and para-sympathetic nervous systems	1
MSE up to scale3 –(<i>MSE1,MSE2,MSE3, MSE1~3</i>)	Matching patterns within parameter series	4
Shannon entropy (<i>E_Shannon(group)</i>) Group: 4,8,16,32 and 64	Overall distribution of parameter series	5
Turning point ratio (<i>TPR</i>)	Turning points of neighboring parameter series	2

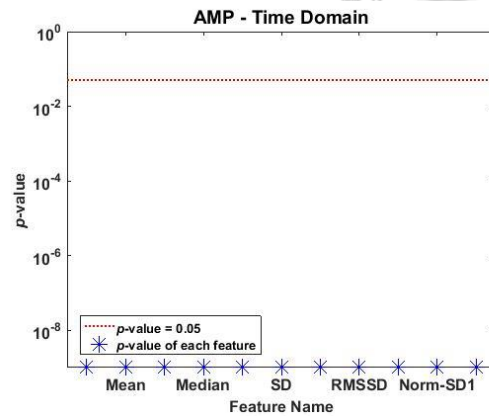
3.5 Statistical Analysis



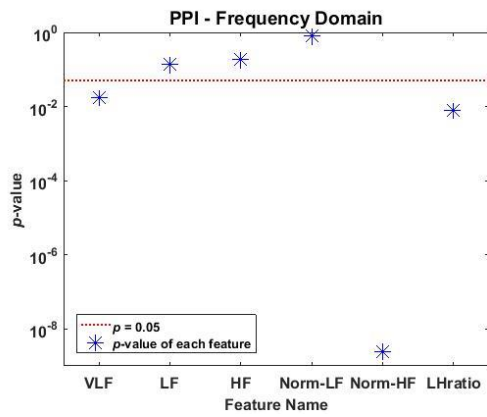
ANOVA is adopted for the statistical analyses of all extracted features. ANOVA calculates p-values by comparing the relative values between the variation within groups and the variation among groups. A common threshold for significant statistical difference is 0.05. The p-values of the extracted features are shown in Fig. 3.15. The lateral axis indicates features name, the vertical axis indicates p-value, which is indicated by a blue star. The common threshold of p-value=0.05 is represented by red line. The blue star under the red line indicates significant statistical difference. Most features show significant statistical differences. Though some frequency domain features show p-value > 0.05. The result suggests the features extracted can be useful for AF detection.



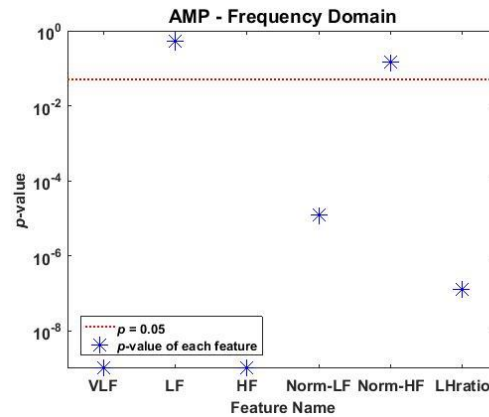
(a)



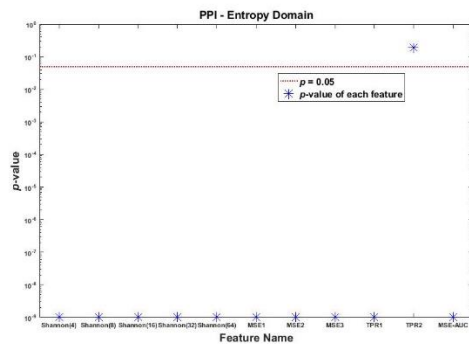
(b)



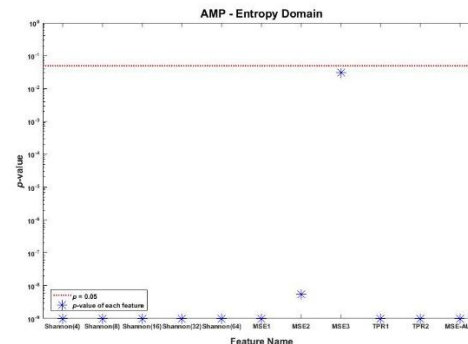
(c)



(d)



(e)



(f)

Fig. 3.15 The p-values of features extracted from PPG (a) PPI - Time domain features, (b) AMP - Time domain features, (c) PPI - Frequency domain features, (d) AMP - Frequency domain features, (e) PPI - Entropy domain features, and (f) AMP - Entropy domain features

3.6 Summary



In this chapter, the flowchart of the proposed framework and the processing part of the proposed framework, including pre-processing, baseline removal and feature extraction are introduced. The proposed pre-processing considering baseline can be applied to PPG signals with baseline wandering, making the framework more robust. And the statistical analysis of features shows significant statistical differences. As a result, the features extracted can be useful for AF detection.

ANOVA is a widely used statistical method which decides whether the differences among groups are significant or not. However, through such a statistical method, we still cannot tell a feature should be selected in the framework and what are the more important features. Therefore, further learning methods are needed, which will be introduced in Chapter 4.



Chapter 4

Classification and Optimization of PPG-based AF Detection

In this chapter, we will introduce the classification part of the proposed framework, including feature selection, classification, and optimization, as shown in Fig. 4.1. First, the traditional feature selection and classification will be introduced as the traditional solution. Then the optimization with GA algorithm is applied in the final proposed framework to enhance the performance even more.

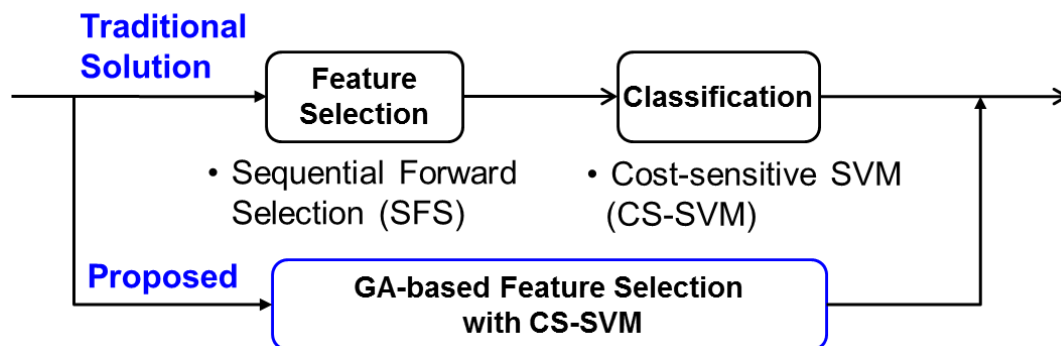
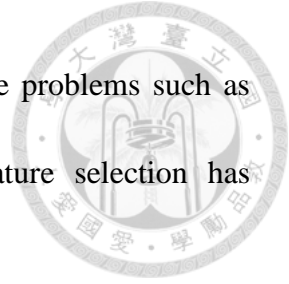


Fig. 4.1 Flow chart of classification part

4.1 Feature Selection

We have $28 \times 2 = 56$ candidate features in the proposed PPG based framework. However, the combination of the features to achieve decent performance is unknown.



Using all the extracted features into a classifier will result in some problems such as “curse of dimensionality” and over-fitting [38]. Performing feature selection has advantages of:

1. Dimension reduction and avoiding over-fitting
2. Finding the dominant features for AF detection
3. Potential higher accuracy and less features in implementation

Analysis of variance (ANOVA) can select the feature with $p\text{-value} < 0.05$ in a common way. However, most features have $p\text{-value} < 0.05$, making ANOVA inefficient in this case. The straightforward method is exhaustive search. However, if we want to select M features as subset from N features, exhaustive evaluation of feature subsets involves $\binom{N}{M}$ and 2^N if M needs to be optimized, too. The amount of combination is too large to implement if the total feature number N is large. Therefore, we applied wrapper type feature selection to find the decent features combination. The famous sequential feature selection algorithm is chosen to find the best features heuristically [39]. Sequential feature selection including sequential forward selection (SFS) and sequential backward selection (SBS). The concept of feature selection and is shown in Fig. 4.2. The steps of SFS/SBS in selecting subset Y_0 from $\{x_1, \dots, x_N\}$ can be



simplified as Table 4-1.

In traditional solution, we applied sequential forward selection to find the feature subset to find the smallest feature subset with best score, defined by accuracy.

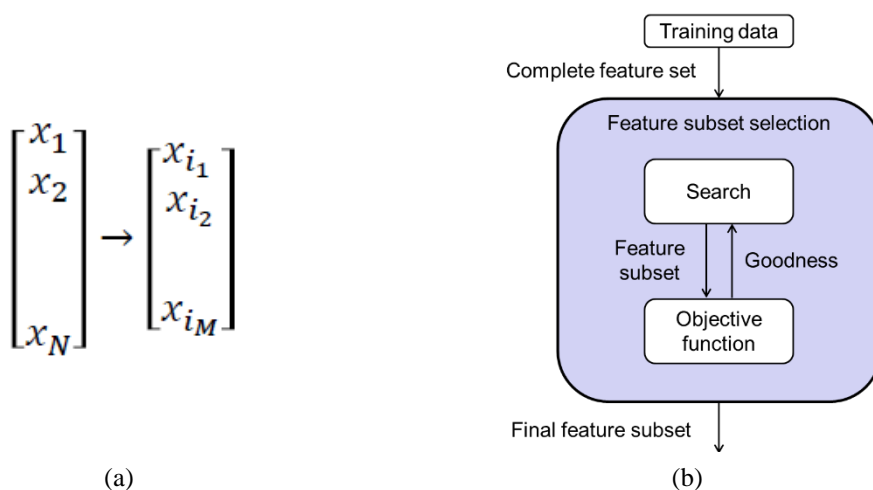


Fig. 4.2 (a) Concept of feature selection, and (b) Concept of wrapper type feature selection [39]

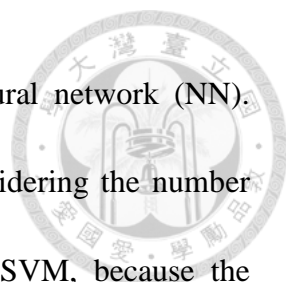
Table 4-1 Steps of sequential forward selection (SFS) and sequential backward selection (SBS)

Steps
S1. Start with the empty set: $Y_0 = \{\emptyset\} / Y_0 = \{x_i i = 1, \dots, N\}$.
S2. Select the next best / worst feature: $x^+ = \arg \max_{x \notin Y_k} J(Y_k + x)$.
S3. Update feature subset: $Y_{k+1} = Y_k + / - x^+; k = k + 1$.
S4. Go to 2, until stop criteria meets.

4.2 Classification

4.2.1 Classification and parameter tuning

There are different techniques for data classification, such as naive Bayes



classifier, random forest, support vector machine (SVM) and neural network (NN). SVM is the classification technique adopted in our experiment considering the number and the properties of our samples. Linear kernel is adopted in SVM, because the performance of RBF kernel is not significantly better than linear kernel. The problem is more linear separable. The features extracted were linear scaled to avoid features with large value dominate the classification. And stratified 5-fold cross-validation is applied to avoid over-fitting in evaluation, as shown in Fig. 4.3. Among 673 subjects, only 151 of them are AF and 522 of them are non-AF, and the AF class is more important in pre-screening. Therefore, we encountered class imbalance problem. The “class imbalance problem” occurs due to the ratio between majority and minority class in the dataset and leads to lower sensitivity. It is a very common problem in practice [40]. Furthermore, the minority class is more important in most cases. Therefore, a cost-sensitive method is adopted to deal with the class imbalance problem.

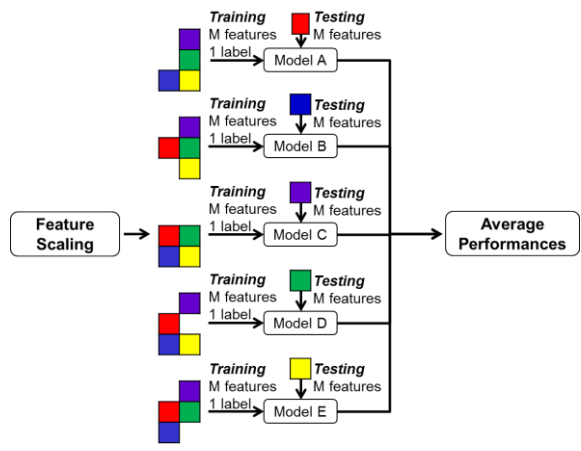


Fig. 4.3 The flow of classification with 5-fold cross-validation



For a separable case, SVM finds the decision boundary by solving the following optimization problem:

$$\min_{\mathbf{w}, b, \xi} \left(\frac{\|\mathbf{w}\|^2}{2} + C \sum_{i=1}^l \xi_i \right), \quad (4.1)$$

where $\xi_i > 0$ corresponds to the slack variable for the i^{th} sample; $C > 0$ is the cost of misclassifying the samples. The cost-sensitive SVM [41] is implemented by modifying the cost of the minority class (positive class label as ξ_i^+) to $C * W$, where W is the penalty weight > 1 and the cost of the majority class (negative class label as ξ_i^-) to C .

The optimization equation is modified as:

$$\min_{\mathbf{w}, b, \xi} \left(\frac{\|\mathbf{w}\|^2}{2} + CW \sum_{i=1}^{l^+} \xi_i^+ + C \sum_{i=1}^{l^-} \xi_i^- \right). \quad (4.2)$$

In traditional solution, we performed the grid search on cost (C) and penalty weight (W) to find the best combination for highest score, defined by sensitivity + specificity. The cost (C) were searched on exponential order ($2^{-4.5} \sim 2^5$) and penalty weight (W) were search on linear order (1~10). And we applied five-fold cross validation to avoid over-fitting in learning. The whole SVM procedure and grid search algorithm is supported by the famous machine learning toolbox LIBSVM [42].



4.2.2 Performance and summary of traditional solution

To evaluate and compare the performances of the proposed framework with related work, the accuracy, sensitivity, specificity, positive predictive value (PPV), negative predictive value (NPV), and receiver operating characteristic (ROC) curve of the frameworks are calculated based on the definitions of confusion matrix shown in Fig. 4.4.

The predicted class refers to the prediction results of the AF detection framework. The actual class refers to the AF or Non-AF labeled doctors. In our experiment, AF is defined as positive class and Non-AF is defined as negative class. Because, the aimed application is screening tool, the AF class (sensitivity) is more important. The result of grid search is shown in Fig. 4.5. The final SVM parameters cost (C) and penalty weight (W) are the ones with best score, defined as sensitivity + specificity.

		Actual Class		
		+	-	
Predicted Class	+	True positive (TP)	False positive (FP)	$TP/(TP+FP)$ = PPV = Precision
	-	False negative (FN)	True negative (TN)	$TN/(TN+FN)$ = NPV
		$TP/(TP+FN)$ = Sensitivity = Recall	$TN/(TN+FP)$ = Specificity	$(TP+TN)/total$ = Accuracy

Fig. 4.4 Confusion matrix

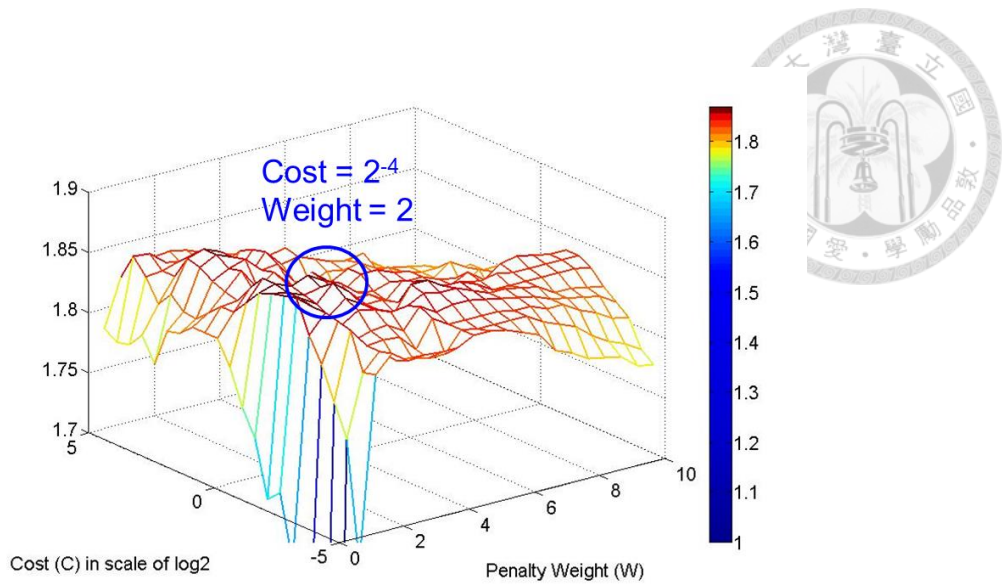


Fig. 4.5 The result of grid search

The traditional solution illustrated in Sec.4.1 and Sec.4.2 is the first solution of the AF detection framework. The comparisons with related works are shown in Table 4-2. The result suggests that framework with traditional solution has better performance than the related works. The result was accepted in IEEE BioCAS, 2016 [43].

Table 4-2 Performance comparisons in traditional solution and related work

	Accuracy	Sensitivity	Specificity	PPV	NPV	ROC_AUC
BioCAS 2016	0.966	0.940	0.973	0.910	0.983	0.968
Related work [20]	0.911	0.848	0.929	0.776	0.955	0.938

4.2.3 Limitations in traditional solution

However, there are limitations in traditional solution. The feature selection



focuses on optimizing feature subset. The SVM parameter, cost (C) and penalty weight (W) are set to default in the process. On the other hand, the parameter tuning focus on optimizing SVM parameter, feature subset is fixed in the process. So traditional solution is not the best optimized feature subset and SVM parameters. The SVM outcome can be simplified as:

$$SVM(features_{subset}, parameter_{SVM}). \quad (4.3)$$

The desired algorithm should be able to optimize feature subset and SVM parameter jointly, will be introduced in next session.

4.3 Features and Classifier Parameters Optimization with GA-based Algorithms

4.3.1 Introduction to GA Algorithms

The Genetic Algorithm (GA) is originated from Darwin's Survival of the fittest [44]. GA was first introduced by John Holland to investigate the usage of the Darwinian senses on computer programs [45]. The GA methodology is particularly suited for optimization, a problem solving technique in which good solutions are searched for in a large solution space. GA can reduce the search complexity by imitating generation



evolution in Darwinian way.

The simple GA flow chart is shown in Fig. 4.6. In GA algorithms, all candidate solutions are regarded as the population in a generation. The structures of a solution are regarded as chromosome, which are often the input of a problem to be optimized. The chromosomes are often design in binary forms. The evaluation of candidate solutions is done using some measures of goodness or fitness, often are the problems to be optimized. After the evaluation, the solutions with poor outcomes are discarded, producing a new generation through mutation. The mutation is carried out by point mutation, cross over and the best solutions in the generation, as shown in Fig. 4.7.

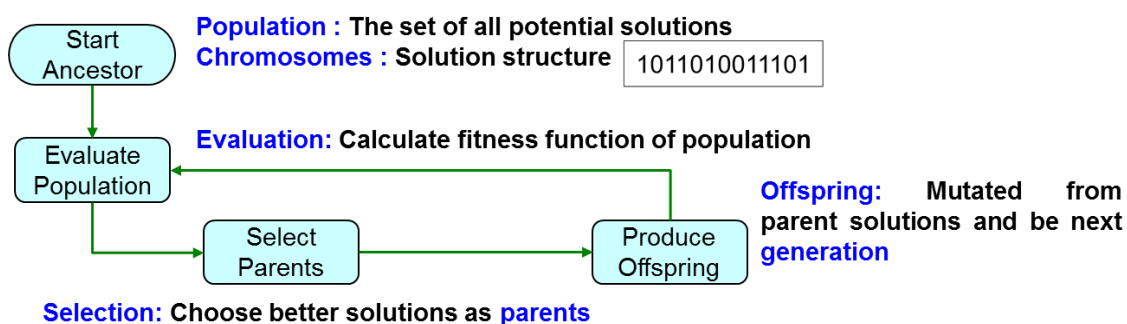


Fig. 4.6 The simple flow chart of GA algorithms

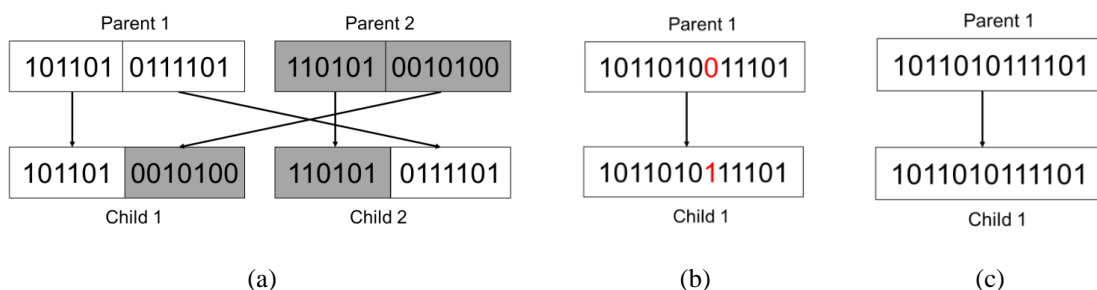


Fig. 4.7 The mutation methods



4.3.2 Optimization with GA Algorithms

The limitations in traditional solution, mentioned in Sec.4.2.3, should be further improved by GA algorithms and optimization. The problem to be optimized is equation (4.3): $SVM(features_{subset}, parameter_{SVM})$. The structure is composed of $features_{subset}$, and $parameter_{SVM}$, both to be optimized jointly to solve the limitation in traditional solution. The solution structure, regarded as the chromosome in GA algorithms is shown in Fig. 4.8. The cost (C) and penalty weight (W) are transferred to binary form in their range of grid search in Sec.4.2.1. And feature subsets are transformed into the feature mask. The selected features are 1 on the index of the feature mask, while the discarded features are 0 on the index of feature mask.

The most important accuracy criteria are sensitivity and ROC's area under curve (ROC_AUC). The optimized is the solution with best score. The evaluation of fitness is defined by:

$$Fitness = 1.5 \text{ sensitivity} + \text{specificity} + PPV + NPV + ROC_AUC \quad (4.4)$$

The proposed GA-based selection with cost-sensitive SVM (CS-SVM) can further improved traditional solution. The algorithm combines feature selection, CS-SVM and evaluation by 5-fold cross-validation, shown in Fig. 4.9.

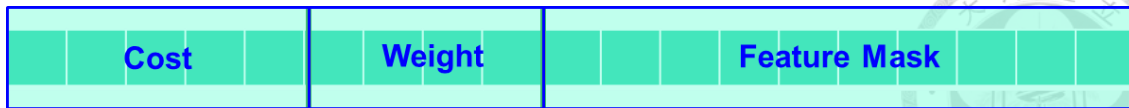


Fig. 4.8 The chromosomes, solution structure

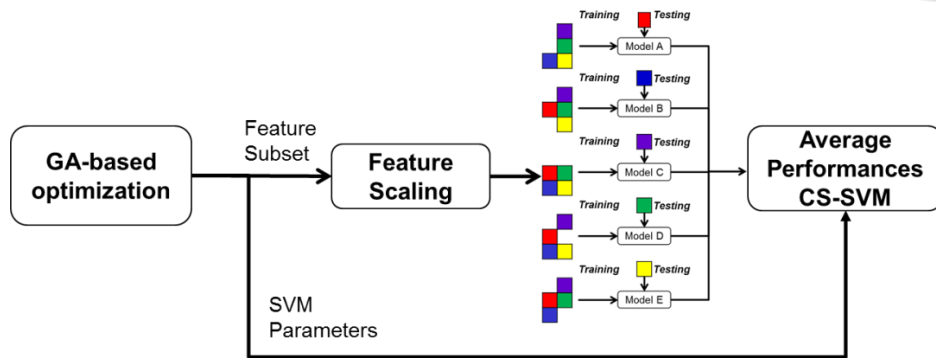


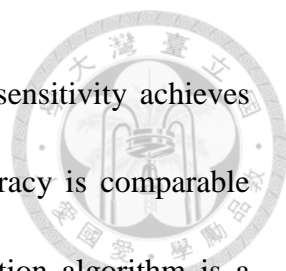
Fig. 4.9 The proposed GA-based optimization with cost-sensitive SVM

4.4 Results of the PPG-based AF Detection Framework

4.4.1 Performance comparisons

To compare our proposed framework with the related works [20], a basis for comparison is needed. Our experiment data are collected in the ICU, the real clinical scenario. We applied their proposed feature RMSSD, Shannon entropy and TPR of PPI on our database to repeat their performance. The traditional solution is also compared to the final framework. The performance comparisons are shown in Table 4-3. And the ROC curve comparisons is shown in Fig. 4.10.

The result suggests that the proposed AF detection framework has better



performance than the related works and traditional solution. The sensitivity achieves 95.4%, and the ROC area under curve achieves 98.0%. The accuracy is comparable EKG-based algorithms and proves that the PPG-based AF detection algorithm is a promising pre-screening tool to help doctors monitoring patient with AF.

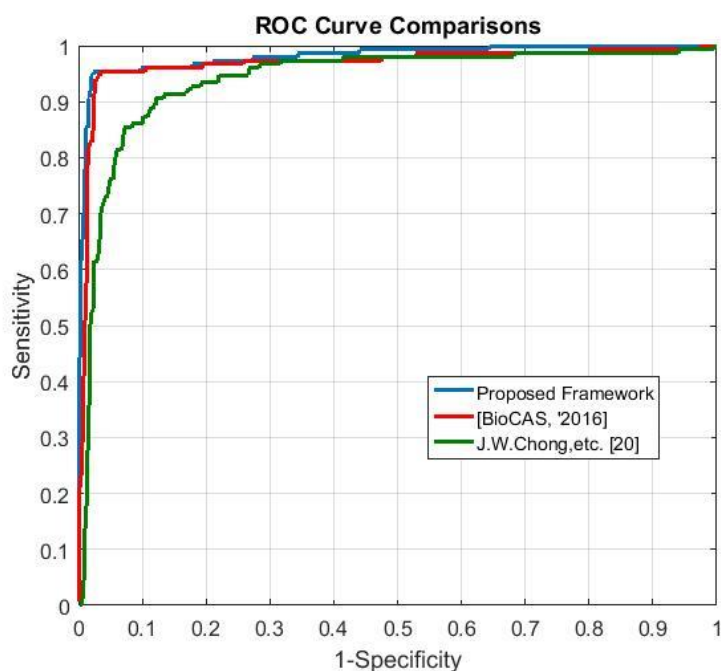


Fig. 4.10 ROC curve comparisons

Table 4-3 The performance comparisons

	Accuracy	Sensitivity	Specificity	PPV	NPV	ROC_AUC
Proposed Framework	0.973	0.954	0.979	0.929	0.987	0.980
BioCAS, '2016	0.966	0.940	0.973	0.910	0.983	0.968
J.W.Chong ,etc. [20]	0.911	0.848	0.929	0.776	0.955	0.938



4.4.2 Features selected in the proposed framework

Furthermore, the feature selected in the GA-based optimization is shown in Table 4-4. This result suggests that utilizing amplitude in the analysis helps the performance of AF detection, since some of the AMP features are selected over PPI features. The number of features are reduced to 16, which is far less than the number of features with p-value <0.05 in the statistical analysis. The blue and bold ones are the features proposed or modified in Sec.3.4 feature extraction. This result further proves the importance of the features proposed or modified in the framework and the importance of feature variety.

Table 4-4 The feature selected in the proposed framework

Category	Selected Features
PPG-PPI	Mean, SD, pNNR(1.1) , pNNR(1.5) , LF, LH Ratio, E_Shannon(4) , MSE1 , TPR1 .
PPG-AMP	Mean, SD, Normalized RMSSD, Normalized HF, LH Ratio, E_Shannon(8) , TPR1 , TPR2 .

4.4.3 Validation within ICU data

The classification accuracy is optimized to find the best SVM parameters and feature subset. Using all data in the optimization is for finding the best model for framework. However, a part of data should be the test set for an even more reliable

accuracy. The concept of test set is shown in Fig. 4.11.

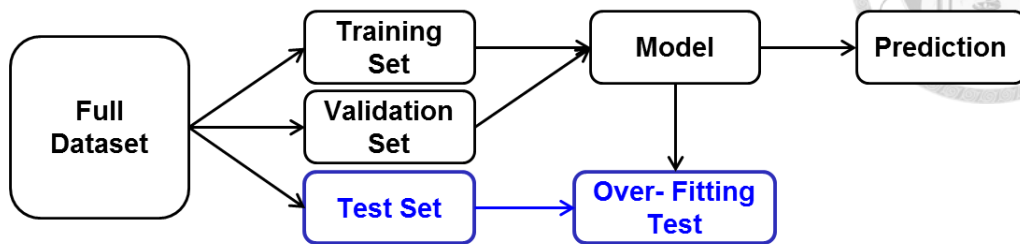


Fig. 4.11 The concept of over-fitting test

In the experiment, the last received data (2015/6-2015/11), are used as test set. This part of data are not including in the optimization. Instead, the data are for testing by the model created by the rest part of data. The test set accuracy compared to the optimized accuracy is shown in Table 4-5. The test set accuracy still shows comparable performance to the optimized accuracy. The validation result further proves the reliability of the proposed framework.

Table 4-5 Test set accuracy compared to the optimized accuracy

	Accuracy	Sensitivity	Specificity	PPV	NPV
Optimized Accuracy	0.973	0.954	0.979	0.929	0.987
Test Set Accuracy	0.951	0.941	0.955	0.889	0.977

4.5 Summary



In this chapter, we introduced the classification part of the proposed framework, including feature selection, classification, and optimization. The comparison results suggest that the proposed PPG-based AF detection framework has better performance than related works and the traditional solution. The algorithmic parts are introduced in Chapter 3 and Chapter 4. On the other hand, the applications of AF detection are shown in the next chapter. The result and performance of the aimed applications of this thesis, including fast screening and long-term monitoring will be introduced.



Chapter 5

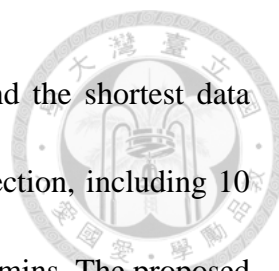
Application of PPG-based AF Detection

In this chapter, we will introduce the application of AF detection. The aimed applications of this thesis include two clinical scenarios, long-term monitoring and fast screening. The PPG-based AF detection framework can be used as a pre-screening tool to assist doctors. On the other hand, the framework can be used for long-term monitoring suspected AF patients. The concepts of fast screening and long-term monitoring have been mentioned in Sec.1.2.2, and shown in Fig. 1.6 and Fig. 1.7.

5.1 Results of Application: Fast Screening and Long-term Monitoring

5.1.1 Fast screening

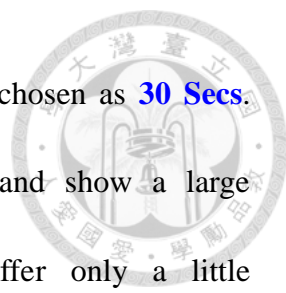
The framework can be used as a screening tool to assist doctors. The aim of fast-screening is to detect whether an individual has AF with very short recording of signals. The fast screening experiment is conducted by manipulating the data length used in the data collection part. As mentioned in Sec.3.2, the data length issue in fast



screening is a trade-off between accuracy and convenience. To find the shortest data length, we experimented with different data length in the data collection, including 10 secs, 20 secs, 30 secs, 40 secs, 1 min, 2 mins, 3 mins, 5 mins and 10 mins. The proposed AF detection framework's performances on different data length are shown in Table 5-1.

Table 5-1 Performances on different data length

	Accuracy	Sensitivity	Specificity	PPV	NPV	ROC_AUC
10 Sec	0.873	0.893	0.868	0.662	0.965	0.906
20 Sec	0.946	0.927	0.952	0.848	0.978	0.959
30 Sec	0.966	0.920	0.979	0.926	0.977	0.968
40 Sec	0.969	0.927	0.981	0.933	0.979	0.970
1 Min	0.973	0.940	0.983	0.940	0.983	0.971
2 Min	0.973	0.954	0.979	0.929	0.987	0.980
3 Min	0.978	0.954	0.985	0.947	0.987	0.977
5 Min	0.981	0.947	0.990	0.966	0.985	0.977
10 Min	0.981	0.954	0.989	0.960	0.987	0.981



According to Table 5-1, the data length of fast-screening is chosen as **30 Secs**. Because the PPVs in under 20 Secs version perform poorly and show a large performance drop. The fast screening version framework suffer only a little performance degrade compared to the more accurate versions. The most important accuracy criteria are sensitivity and ROC's area under curve (ROC_AUC). Judging mainly from these 2 criteria, the performances become stable when data length > 2mins. In conclusion, the version with data length > **2mins** can be regarded as accurate model and applied on long-term monitoring.

5.1.2 Long-term monitoring

The aim of long-term monitoring is to precisely detect paroxysmal AF patient and find the duration of AF to assist doctors' decision of treatment. According to Table 5-1, the 2 mins version framework is applied. The framework can be applied on long-term monitoring by make a decision of AF or non AF every 2 mins. The decision of the proposed PPG-based framework are compared to the EKG-based framework. To evaluate the similarity between two prediction results of the frameworks, the simple matching coefficient (SMC) is calculated:

$$SMC = (M_{11} + M_{00}) \div (M_{11} + M_{10} + M_{01} + M_{00}), \quad (5.1)$$



where M_{11} , M_{10} , M_{01} , and M_{00} refer to the number of decisions made by PPG-based framework and EKG-based framework are (1,1), (1,0), (0,1), and (0,0), respectively.

And the ratio of the whole recording are also calculated.

$$AF\ ratio = \frac{AF}{AF+NAF} \quad (5.2)$$

The case studies of some patients with long-term data (6-8 hours) are as follows:

1. ID=2956355, the result is shown in Fig. 5.1(a) and Fig. 5.1(b). The result suggests that the patient is **Non-AF**. And the SMC between EKG-based framework and PPG-based framework is **100%**.

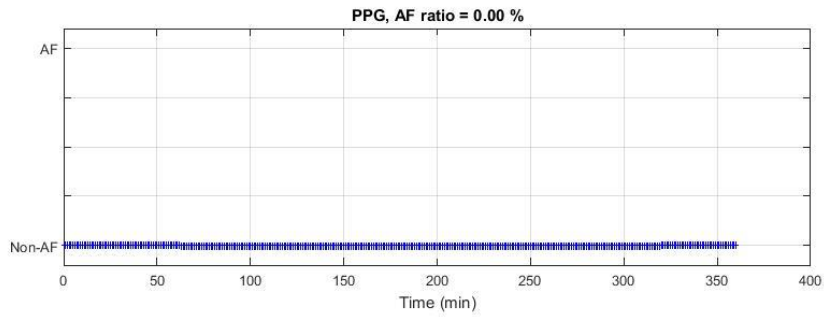
2. ID=3234202, the result is shown in Fig. 5.1(c) and Fig. 5.1(d). The result suggests that the patient is **persistent AF**. And The SMC between EKG-based framework and PPG-based framework is **100%**.

3. ID=5302261, the result is shown in Fig. 5.1(e) and Fig. 5.1(f). The result suggests that the patient is **paroxysmal AF**. And The SMC between EKG-based framework and PPG-based framework is **89.88%**.

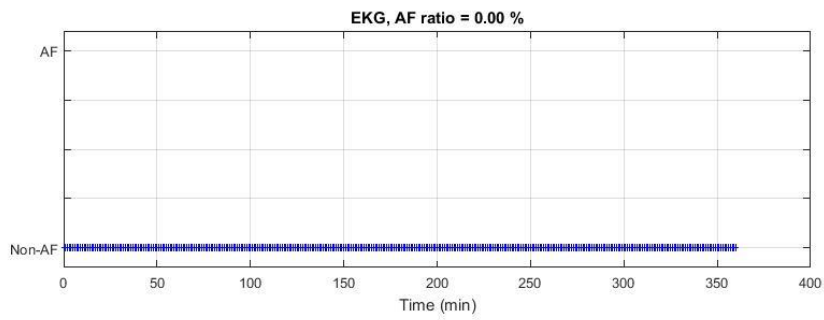
4. ID=5650186, the result is shown in Fig. 5.1(g) and Fig. 5.1(h). The result suggests that the patient is **paroxysmal AF**. And The SMC between EKG-based framework and PPG-based framework is **97.08%**.



ID = 2956355 , SMC = 100.00 %

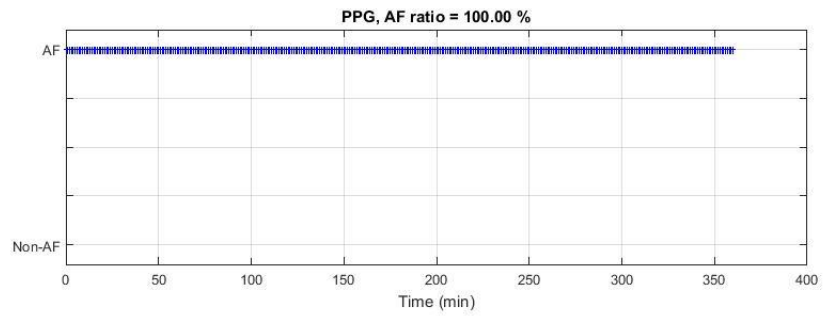


(a)

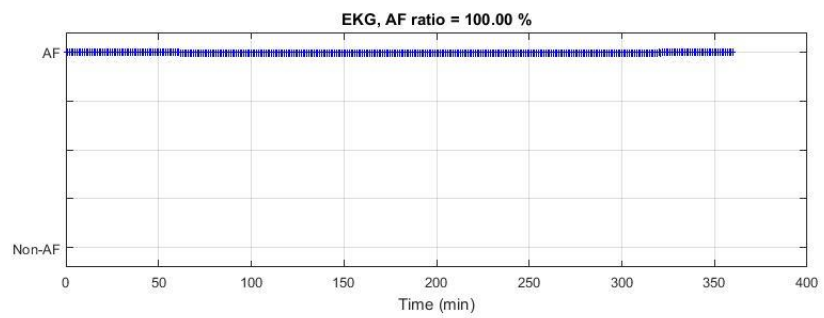


(b)

ID = 3234202 , SMC = 100.00 %



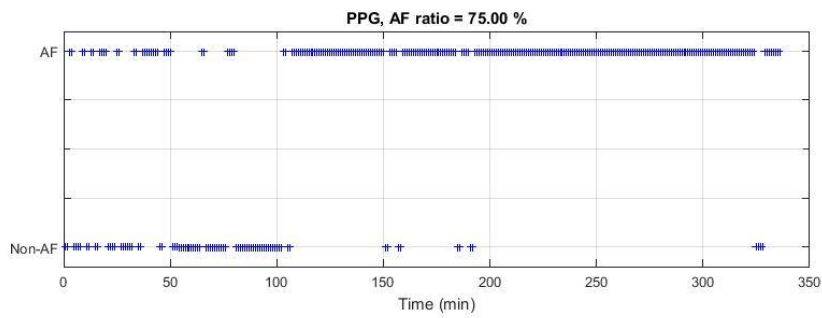
(c)



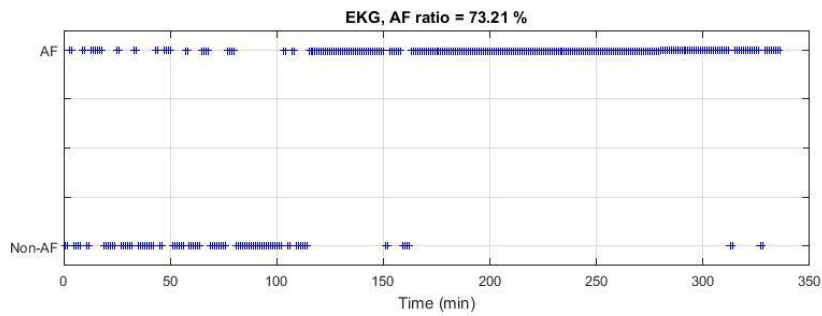
(d)



ID = 5302261 , SMC = 89.88 %

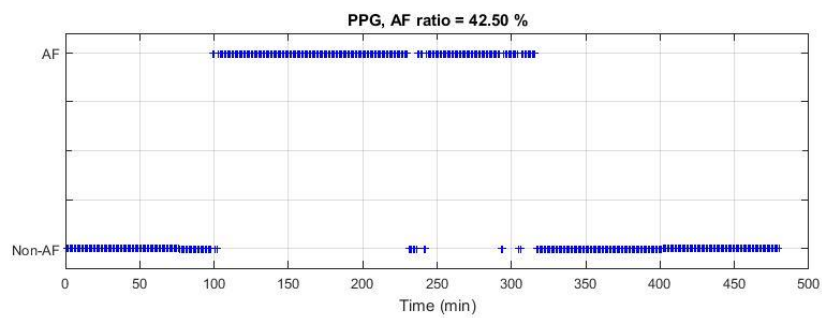


(e)

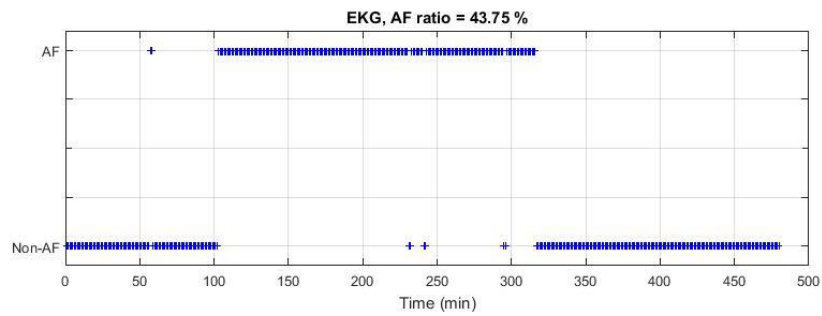


(f)

ID = 5650186 , SMC = 97.08 %

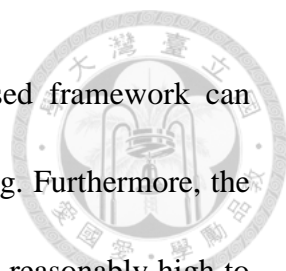


(g)



(h)

Fig. 5.1 Long-term monitoring result of patient (a) ID=2956355 PPG, (b) ID=2956355 EKG, (c) ID=3234202 PPG, (d) ID=3234202 EKG, (e) ID=5302261 PPG, (f) ID=5302261 EKG, (g) ID=5650186 PPG, and (h) ID=5650186 EKG

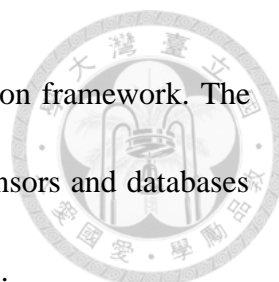


The above case studies suggest that the proposed PPG-based framework can detect paroxysmal AF and find the AF ratio of a long-term recording. Furthermore, the SMC between EKG-based framework and PPG-based framework is reasonably high to suggest that PPG signals are potential to replace EKG signals in long-term AF detection.

5.2 Validation on MTK Device

The results shown are based on ICU data so far. However, the validation with different data base is needed to further strengthen the reliability of the framework. And the implementation of GUI can make the framework easy accessed by medical staffs. The project is supported by: National Taiwan University (NTU) - National Taiwan University Hospital (NTUH) - MediaTek Innovative Medical Electronics Research Center. The trial experiment with MTK devices is important to preview the potential of using MTK devices to record PPG signals for AF detection.

The data received from MTK watch MT2511, as shown in Fig. 5.2, are used for validation in the framework. MT2511 is a prototype wrist-type PPG and EKG sensor. 20 patients in ICU were tested, whose EKG and PPG signals were recorded by MT2511 for 2 minutes. The signals were transferred to the android phone with Bluetooth and processed in the PC and the amplitude units were scaled into database scales. The



signals were then processed by the proposed PPG-based AF detection framework. The experiment can validate the utility of the framework on different sensors and databases and further prove the possibility of AF detection on wearable devices.

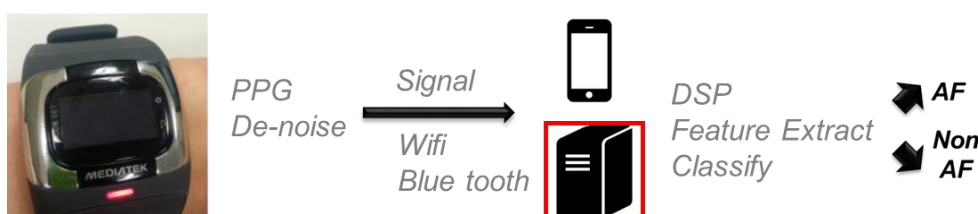


Fig. 5.2 Adopted from MediaTek. The flow chart of applied MT2511 in validation

Among the 24 patients, 11 of them were found to be AF by doctors while recording. These PPG signals were processed by the proposed AF detection framework (accurate model) and 30 secs version framework (fast screening). The result is shown in Table 5-2. Though the database is not large in the trial experiment, the result suggests that the framework is able to be applied on MT2511. And the result shows the potential of AF detection base on PPG signals with wearable devices.

Table 5-2 The trial validation on MTK devices, MT2511

	Accuracy	Sensitivity	Specificity
Fast screening (30 secs)	24/24=100%	11/11=100%	13/13=100%
Accurate model (2 mins)	24/24=100%	11/11=100%	13/13=100%

5.3 Implementation of Graphic User Interface

The framework has potential to be applied to real clinical uses. For the

convenience of medical staffs, the implementation of graphic user interface (GUI) is implemented. The interface of the GUI is shown in Fig. 5.3. The GUI can support both application scenarios, long-term monitoring and fast screening. First, the user should select the file of raw data recorded by the medical devices. Second, the application scenario should be chosen. Third, the parameters, including sampling frequency and the monitoring range from long-term monitoring should be given. Final, the GUI will run program and generate the report by clicking start button.

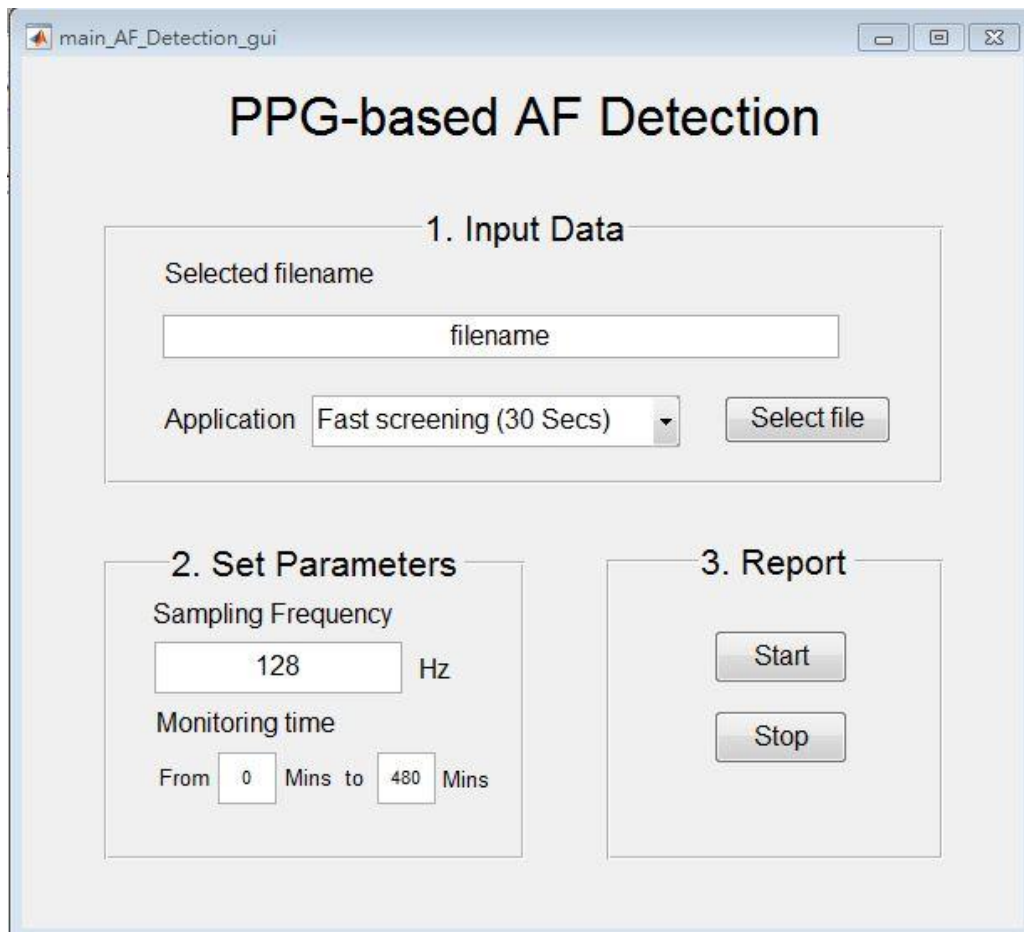
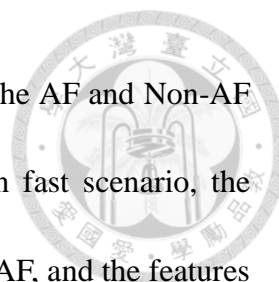


Fig. 5.3 The interface of GUI



In long-term monitoring scenario, the generated report shows the AF and Non-AF of the whole recording and the AF ratio, as shown in Fig. 5.4. In fast scenario, the generated report shows the waveforms, the decision of AF and Non-AF, and the features extracted during the recording, as shown in Fig. 5.5.

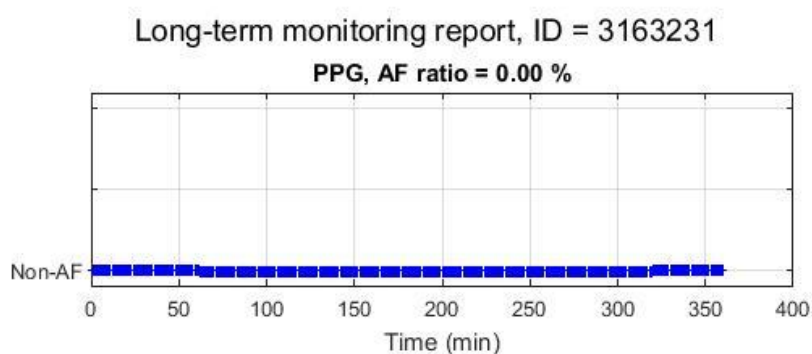


Fig. 5.4 Report of long-term monitoring

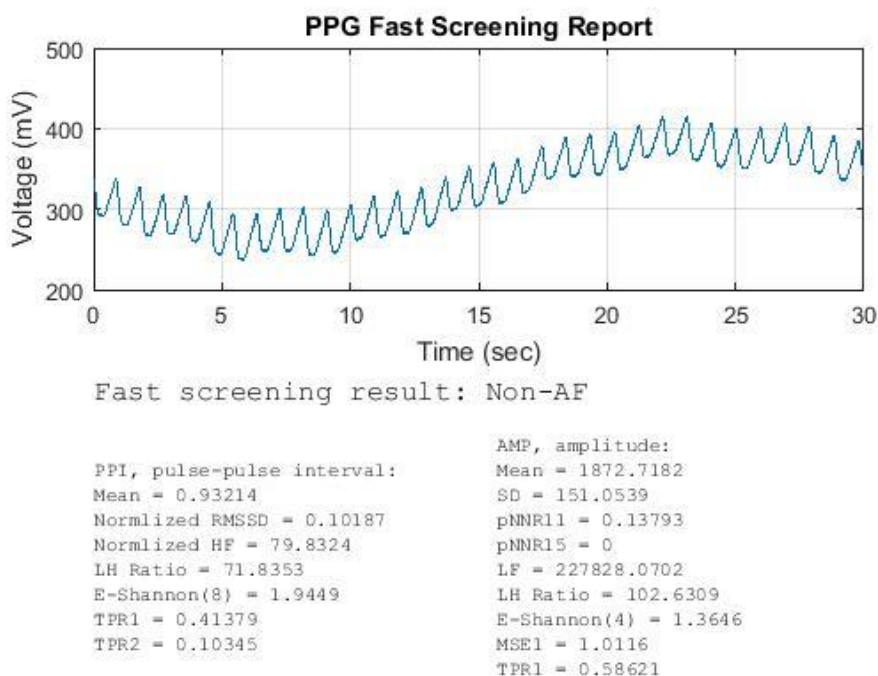


Fig. 5.5 Report of fast-screening

5.4 Summary



In this chapter, we introduced the application of AF detection. The results of the aimed applications of this thesis including fast screening and long-term monitoring are shown. The recording time can be shortened to 30 seconds in fast screening scenario with little performance degradation. And the proposed PPG-based AF detection framework is able to detect paroxysmal AF in long-term monitoring and highly correlated to EKG-based framework. Furthermore, the validation with different data base strengthens the reliability of the framework. Finally, the graphic user interface (GUI) is implemented for the convenience of medical staffs.



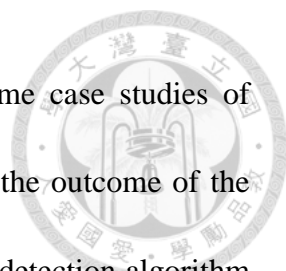
Chapter 6

Conclusion and Future Works

6.1 Main Contribution

In this thesis, the PPG-based AF detection framework is proposed. The drawbacks and limitations of related works are improved in the proposed framework. The framework can be applied to PPG signals with baseline wandering by improved pre-processing. The framework jointly analyzes all the PPG features extracted from AMP and PPI. And more features are considered and even improved in the feature extraction part. Most features show significant statistical difference ($p < 0.05$) in AF detection. In the classification part, the GA-based feature selection with CS-SVM is applied to jointly consider feature selection and the class imbalance problem. Among 673 patients' signals recorded in clinic environments, we achieve ROC area under curve, sensitivity, specificity and accuracy of 0.980, 0.954, 0.979 and 0.973, respectively in cross-validation. The performances are higher than those of the PPG related works. And the accuracy and reliability is validated with MTK devices and within ICU database.

Furthermore, two clinical scenarios, long-term monitoring and fast screening were considered in the experiments. The record time can be shortened to 30 seconds with




little performance degradation in fast screening scenario. And some case studies of long-term monitoring are shown, which are highly correlated with the outcome of the EKG-based framework. The result suggests that the PPG-based AF detection algorithm is a promising pre-screening tool for AF and helps doctors monitoring patient with AF.

Partial work of this thesis was submitted and accepted in EE conference, *IEEE BioCAS*, 2016 and medical journal, *Nature Scientific Reports*, 2017.

6.2 Future Works

The main limitation of the proposed framework is that it is based on PPG's parameters, such as PPI and AMP. However, the p-wave in EKG is also a key to diagnose AF. Some patients with AF shows more regular parameters comparing to others, however, the p-wave is absent in EKG. These kinds of patients are misclassified as Non-AF in the framework. The p-wave cannot be shown on PPG, which is the main drawback of PPG-based AF detection and other kinds of heart-beat based AF detection.

In the future, we expect our proposed framework can be integrated with the existing devices in ICU and MTK devices, carrying out the online monitoring of AF detection. Furthermore, we plan to build the processing unit in the local and upload



the information onto the cloud server, reducing overhead of data uploading bandwidth, providing the latest information of patients for medical staff and family members. The online system can screen out potential AF patients and alert the medical staff in advance.

Although the inspection of physiological signals can never replace medical imaging system and doctors' diagnosis, it provides a feasible and quantitative way to monitor without any side effect. To our ambitiousness, the optimal goal is to implement a highly accurate analysis system, which is as accurate as EKG devices. Additionally, this framework is not able to investigate other kinds of arrhythmia because the lack of corresponding data. The ability to diagnosis other kinds of arrhythmia such as PVC and PAV is also a good future direction of the thesis.

Reference



[1] National Institutes of Health (NIH).

<http://www.nhlbi.nih.gov/health/health-topics/topics/af>

[2] Hamilton Cardiology Associate.

<https://www.hcahamilton.com/atrial-fibrillation>

[3] The Internet Stroke Center.

<http://www.strokecenter.org/patients/about-stroke/what-is-a-stroke>

[4] American Heart Association.

http://www.heart.org/HEARTORG/Conditions/Arrhythmia/AboutArrhythmia/Atrial-Fibrillation-AF-or-AFib_UCM_302027_Article.jsp#.WMCR2m995ph

[5] C. Gutierrez, D. Blanchard "Atrial Fibrillation: Diagnosis and Treatment", in *Am Fam Physician*. 2011; 83 (1): 61–68.

[6] F. Valentin, "ACC/AHA/ESC 2006 Guidelines for the Management of Patients with Atrial Fibrillation: a report of the American College of Cardiology/American Heart Association Task Force on Practice Guidelines and the European Society of Cardiology Committee for Practice Guidelines: developed in collaboration with the European Heart Rhythm Association and the Heart Rhythm Society", in *Circulation*. 2006; 114: e257–354.

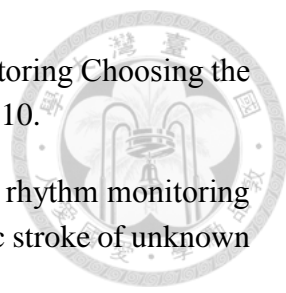
[7] Gladstone, D. J., Spring, M., Dorian, P., et al., "Atrial fibrillation in patients with cryptogenic stroke," in *New England Journal of Medicine*, vol. 370, no. 26, pp. 2467-2477, 2014.

[8] Phillips monitors

<http://www.philips.com.tw/healthcare/solutions/patient-monitoring/>

[9] Medtronics

<http://www.medtronic.com/us-en/about/news/media-resources/media-kits/seeq-mobile-cardiac-telemetry-system.html>

- 
- [10] Zimetbaum, P. and Goldman, A, “Ambulatory Arrhythmia Monitoring Choosing the Right Device,” in *Circulation*, vol. 122, no. 16, pp. 1629-1636, 2010.
- [11] Seet, R. C., Friedman, P. A., and Rabinstein, A. A., “Prolonged rhythm monitoring for the detection of occult paroxysmal atrial fibrillation in ischemic stroke of unknown cause,” in *Circulation*, vol. 124, no. 4, pp. 477-486, 2011.
- [12] T. Tamura, Y. Maeda, M. Sekine and M. Yoshida. “Wearable Photoplethysmographic Sensors—Past and Present,” in *Electronics*, 2014.
- [13] Texas instrument
- <http://www.ti.com/tool/tida-00011>
- [14] Chan PH, Wong CK, Poh YC, Pun L, Leung WWC, Wong YF, Wong MMY, Poh MZ, Chu DWS, Siu CW, “Diagnostic performance of a smartphone - based photoplethysmographic application for atrial fibrillation screening in a primary care setting,” in *J Am Heart Assoc*. 2016
- [15] Larburu, N., Lopetegi, T., and Romero, I., “Comparative study of algorithms for atrial fibrillation detection,” in *IEEE Computing in Cardiology*, pp. 265-268, Sep. 2011.
- [16] Tatento K, Glass L. “Automatic detection of atrial fibrillation using the coefficient of variation and density histograms of RR and RR intervals.” in *Medical & Biological Engineering & Computing* 2001; 39: 664-671.
- [17] Lee, J., Reyes, B. A., McManus, D. D., et al., “Atrial fibrillation detection using a smart phone,” in *IEEE Annual International Conference on Engineering in Medicine and Biology Society (EMBC)*, pp. 1177-1180, Aug. 2012.
- [18] Jinseok, L., Reyes, B.A., McManus, D.D., and Mathias, O., “Atrial fibrillation detection using an iPhone 4S,” in *IEEE Transactions on Biomedical Engineering*, vol. 60, no. 1, pp. 203-206., Jan. 2013.
- [19] McManus, D. D., Lee, J., Maitas, O., et al., “A novel application for the detection of an irregular pulse using an iPhone 4S in patients with atrial fibrillation,” in *Heart rhythm: the official journal of the Heart Rhythm Society*, vol. 10, no. 3, pp. 315-319, Mar. 2013.
- [20] J. W. Chong, N. Esa, D. D. McManus and K. H. Chon, "Arrhythmia Discrimination Using a Smart Phone," in *IEEE Journal of Biomedical and Health Informatics*, vol. 19,

no. 3, pp. 815-824, May 2015.

[21] Khan, M. and Miller, D. J., "Detection of paroxysmal atrial fibrillation in stroke/tia patients," in *Stroke research and treatment*, 2013.

[22] Ming-zher Poh, "Method and system for screening of atrial fibrillation" US patent, US 20150359443 A1, 12/17/2015.

[23] Kardia mobile, AliveCor, Inc.

<https://www.alivecor.com/en>

[24] J. Pan and W. J. Tompkins, "A Real-Time QRS Detection Algorithm," in *IEEE Transactions on Biomedical Engineering*, vol. BME-32, no. 3, pp. 230-236, March 1985.

[25] M. Di Rienzo, P. Castiglioni, and G. Parati, "Arterial blood pressure processing," in *Wiley Encyclopedia of Biomedical Engineering*, Apr 2006.

[26] D. J. Meredith, D. Clifton, P. Charlton, J. Brooks, C. W. Pugh and L. Tarassenko, "Photoplethysmographic derivation of respiratory rate: a review of relevant physiology" in *Journal of Medical Engineering & Technology*, 2012.


[27] D. J. Jang, et al, "A Robust Method for Pulse Peak Determination in A Digital Volume Pulse Waveform with A Wandering Baseline," in *IEEE Trans. Biomed. Circuits Syst.*, vol.8, no.5, pp.729-737, 2014.

[28] K. A. Reddy and V. J. Kumar. "Motion Artifact Reduction in Photoplethysmographic Signals using Singular Value Decomposition," in *IEEE Instrumentation and Measurement Technology Conference*, MAY, 2007.

[29] K. L. Park, K. J. Lee, and H. R. Yoon, "Application of a wavelet adaptive filter to minimize distortion of the ST-segment," in *Med. Biol. Eng. Comput.*, vol. 36, pp. 581–586, 1998.

[30] B Prathyusha, T Sreekanth Rao, D. Asha, "Extraction of Respiratory Rate From PPG Signals Using PCA and EMD" in *International Journal of Research in Engineering and Technology*, 2012.

[31] P. Sun, Q. H. Wu, A. M. Weindling, et al, "An Improved Morphological Approach to Background Normalization of ECG Signals," in *IEEE Trans. Biomed. Eng.* vol. 50, no. 1, pp. 117-121, 2003.

- 
- [32] Shih, Frank Y, “*Image processing and mathematical morphology: fundamentals and applications*”, CRC Press, c2009, Chap 2.
- [33] Gernot Ernst, “*Heart Rate Variability*” Springer Science & Business Media, 2013, Chapter 4.
- [34] M. Costa, A. L. Goldberger, and C. K. Peng, “Multiscale entropy analysis of biological signals,” *Phys. Rev. E*, vol. 71, pp. 1–17, 2005.
- [35] P. H. Tsai, C. Lin, J. Tsao, “Empirical mode decomposition based detrended sample entropy in electroencephalography for Alzheimer's disease”, in *Journal of Neuroscience Methods*, vol. 210, pp. 230-237, Sep. 2012.
- [36] W. A. Wallis and G. H. Moore, “A Significance Test for Time Series Analysis.” in *Journal of the American Statistical Association*, vol. 36, pp. 401- 409, 1946.
- [37] S. Dash, E. Raeder, S. Merchant and K. Chon, "A statistical approach for accurate detection of atrial fibrillation and flutter," in *Proc, Annual Computers in Cardiology Conference (CinC)*, Sep. 2009, pp. 137-140.
- [38] Saeys, Y., Inza, I., and Larrañaga, P., “A review of feature selection techniques in bioinformatics,” in *Bioinformatics*, vol. 23, no. 19, pp. 2507-2517, Aug. 2007.
- [39] Salt Okunur, CSE802, Michigan state university.
- [40] C. P. Chan and S. Stolfo, “Toward scalable learning with non-uniform class and cost distributions,” in *Proc. Int'l Conf. Knowledge Discovery and Data Mining*, Aug. 1998, pp. 164-168.
- [41] Sun, Y., Wong, A. K., and Kamel, M. S., “Classification of imbalanced data: A review,” in *International Journal of Pattern Recognition and Artificial Intelligence*, vol. 23, no. 4, pp. 687-719, 2009.
- [42] C. C. Chang and C. J. Lin, “LIBSVM : a library for support vector machines,” *ACM Transactions on Intelligent Systems and Technology*, Vol.2, no. 27, pp. 1-27, 2011
- [43] Shih-Ming Shan, Sung-Chun Tang, Pei-Wen Huang, Yu-Min Lin, Wei-Han Huang, Dar-Ming Lai, An-Yeu Wu, "Reliable PPG-based Algorithm in Atrial Fibrillation Detection," in *Proc. IEEE BioMedical Circuits and Systems Conference*, pp. 340-343, Shanghai, China, Oct. 2016.
- [44] Charles Darwin, “*Origin of Species*”, 1859.

[45] John Holland, “*Adaptation in Natural and Artificial Systems*”, M.I.T.P., 1992.

[46] Muhannad Harrim, CS479, Western Michigan University.

[47] Matlab global optimization toolbox.

<https://www.mathworks.com/products/global-optimization.html>

